

Strongly consistent community detection in popularity adjusted block models

Quan Yuan[†], Binghui Liu[†], Danning Li[†] and Lingzhou Xue[‡]

[†] Northeast Normal University

[‡]The Pennsylvania State University

Abstract

The Popularity Adjusted Block Model (PABM) provides a flexible framework for community detection in network data by allowing heterogeneous node popularity across communities. However, this flexibility increases model complexity and raises key unresolved challenges, particularly in effectively adapting spectral clustering techniques and efficiently achieving strong consistency in label recovery. To address these challenges, we first propose the Thresholded Cosine Spectral Clustering (TCSC) algorithm and establish its weak consistency under the PABM. We then introduce the one-step Refined TCSC algorithm and prove that it achieves strong consistency under the PABM, correctly recovering all community labels with high probability. We further show that the two-step Refined TCSC markedly accelerates clustering error convergence, especially with small sample sizes. Additionally, we propose a data-driven approach for selecting the number of communities, which outperforms existing methods under the PABM. The effectiveness and robustness of our methods are validated through extensive simulations and real-world applications.

Keywords: Spectral clustering, One-step refinement, Strong consistency

1 Introduction

Networks provide a powerful tool for representing and analyzing the relationships between interacting units in complex systems (Wasserman and Faust, 1994; Goldenberg et al., 2010). A central problem in network data analysis is community detection, which seeks to partition the nodes of the network into distinct groups or communities. Identifying such communities can yield valuable insights into the network’s underlying organization and structure. A substantial body of research on community detection spans multiple disciplines, including business(Chen et al., 2024), social science (Moody and White, 2003), environmental studies

(Agarwal and Xue, 2020), and genetics (Spirin and Mirny, 2003; Zhang and Cao, 2017). For comprehensive reviews of this topic, see Fortunato (2010); Fortunato and Hric (2016); Kim et al. (2018).

In recent decades, there has been substantial progress in statistical models for community detection with network data. The Erdős–Rényi (ER) random graph model (Erdős and Rényi, 1959) assumes that all node pairs in the network are connected independently with a common edge probability. To accommodate community structure, Holland et al. (1983) proposed the stochastic block model (SBM), in which the n nodes are partitioned into K communities, and the probability of an edge between two nodes depends solely on their community memberships. Specifically, nodes i and j are connected with probability P_{kl} if they belong to communities k and l , respectively, for $i, j \in \{1, \dots, n\}$ and $k, l \in \{1, \dots, K\}$. To account for degree heterogeneity often observed in real-world networks, Karrer and Newman (2011) introduced the degree-corrected stochastic block model (DCSBM), which extends the SBM by assigning each node a degree parameter that uniformly scales its connectivity across all communities, thereby modeling varying node popularity.

Nevertheless, neither the SBM nor the DCSBM adequately captures variations in node popularity across communities, a phenomenon frequently observed in real-world networks. For instance, even if nodes i and j belong to the same community, there may exist communities k and l such that community k exhibits stronger connectivity to node i than to node j , while community l connects more strongly to node j than to node i . To model such asymmetries, Sengupta and Chen (2017) proposed the Popularity Adjusted Block Model (PABM) with parameter matrix $\mathbf{\Lambda} = (\lambda_{i'k'}) \in \mathbb{R}^{n \times K}$, where $\lambda_{i'k'}$ encodes the popularity of node i' with respect to community k' , in which the probability of an edge between nodes i and j —belonging to communities k and l , respectively—is given by $\lambda_{il}\lambda_{jk}$.

Several methods have been proposed for community detection under the PABM. Sengupta and Chen (2017) optimized a modified modularity function and established the weak

consistency of its proposed estimator, namely, as $n \rightarrow \infty$, for any $\varepsilon > 0$,

$$\mathbb{P} \left\{ \min_{\pi: [K] \rightarrow [K]} \frac{1}{n} \sum_{i=1}^n \mathbb{I}\{\mathbf{c}^*(i) \neq \pi(\hat{\mathbf{c}}(i))\} < \varepsilon \right\} \rightarrow 1,$$

where $\hat{\mathbf{c}} \in [K]^n$ is an estimate of the true community label vector \mathbf{c}^* . Subsequently, [Noroozi et al. \(2021a,b\)](#) noted that the structure of the edge probability matrix in the PABM poses challenges for the direct application of spectral clustering. To address this, they proposed an alternative community detection method based on subspace clustering in practice and also proved the weak consistency of their estimator. More recently, [Koo et al. \(2023\)](#) analyzed the PABM within the framework of generalized random dot product graphs and showed that community labels can be recovered with high accuracy, provided that the rows of matrix $\mathbf{\Lambda}$ for nodes within the same community are assumed to be independently and identically distributed (*i.i.d.*). This assumption imposes a stronger constraint than those in [Sengupta and Chen \(2017\)](#) and [Noroozi et al. \(2021b\)](#), and as shown in [Section 5.3](#), when this *i.i.d.* assumption is violated, the performance of its algorithm deteriorates significantly.

Despite the important progress made in developing and analyzing methods for community detection under the PABM, two key open questions remain:

- (1) Can spectral clustering be effectively implemented under the PABM? Spectral methods are widely studied and known for their practical efficiency in community detection. Classical spectral clustering techniques—such as those in [Rohe et al. \(2010\)](#); [Sussman et al. \(2011\)](#); [Lei and Rinaldo \(2015\)](#); [Abbe and Sandon \(2015\)](#); [Su et al. \(2020\)](#)—and their numerous variants—e.g., [Amini et al. \(2013\)](#); [Jin \(2015\)](#); [Huang et al. \(2024\)](#); [Jin et al. \(2024\)](#)—have demonstrated strong empirical performance and theoretical guarantees under various network models. Owing to their computational efficiency, these methods are often used as initialization steps in more complex procedures ([Amini et al., 2013](#); [Gao et al., 2017](#); [Yun and Proutiere, 2016](#); [Wang et al., 2020](#); [Zhao et al., 2024](#)). However, it remains unclear whether such strategies can be effectively adapted to the PABM, given its more flexible and heterogeneous structure.
- (2) Is it possible to efficiently achieve strong consistency for community label estimation under the PABM? As discussed in [Zhao et al. \(2011\)](#), consistency in community

detection can be classified as weak or strong. Strong consistency refers to the exact recovery of all community labels (up to a permutation) with high probability:

$$\mathbb{P} \left\{ \bigcup_{\pi: [K] \rightarrow [K]} (\hat{\mathbf{c}} = \pi[\mathbf{c}^*]) \right\} \rightarrow 1,$$

where $\pi[\mathbf{c}^*] = (\pi(\mathbf{c}^*(1)), \dots, \pi(\mathbf{c}^*(n)))^\top$. A strongly consistent estimation of community labels is particularly valuable in downstream inference tasks. For example, in hypothesis testing for network models (Zhang and Chen, 2017; Yuan et al., 2022) or in estimating the number of communities (Saldana et al., 2017; Chen and Lei, 2018; Li et al., 2020; Hu et al., 2021; Jin et al., 2023), strongly consistent community estimates can be directly incorporated into test statistics, thereby enhancing the reliability and validity of the resulting inference. When the initialization is reasonable, a refinement step often improves estimation accuracy, as shown for SBM (Gao et al., 2017) and DCSBM Gao et al. (2018). However, efficiently refining estimates under the PABM poses significantly greater challenges and remains an open problem.

In this paper, we provide affirmative answers to these two open questions. To address the first, we derive the explicit form of the eigenvector matrix of the PABM’s edge probability matrix (see Proposition 1). This characterization reveals that, unlike in the SBM where the rows of the eigenvector matrix corresponding to nodes within the same community are identical, or in the DCSBM where they are proportional, the PABM exhibits a more intricate structure: rows within the same community are neither identical nor proportional. As a result, standard spectral clustering methods and their variants, such as spherical spectral clustering, are ineffective under the PABM. However, our result suggests that the angle between the representations of nodes in the eigenspace can serve as a meaningful similarity measure. With a simple transformation, we construct a similarity matrix from the eigenspace and apply K-means clustering, following the general principle of standard spectral clustering.

To address the second question, we propose an one-step refinement algorithm based on the inter-cluster angular similarity of the adjacency matrix, specifically designed to enhance the accuracy of community label estimation. Importantly, our approach—consistent with

the modeling assumptions in [Sengupta and Chen \(2017\)](#) and [Noroozi et al. \(2021b\)](#)—does not impose any distributional assumptions on the matrix \mathbf{A} . As demonstrated by the simulation results in [Figure 10](#), this flexibility enables our method to perform well even when the rows of \mathbf{A} are not *i.i.d.*.

Our contributions in this paper are threefold. First, we provide a comprehensive analysis of the eigenspace structure of the edge probability matrix under the PABM. Building on this structural analysis, we develop the Thresholded Cosine Spectral Clustering (TCSC) algorithm, which serves as an effective initialization procedure and yields a weakly consistent estimator of the community labels. Second, we show that one-step Refined TCSC is sufficient to upgrade the weakly consistent estimate to a strongly consistent one, that is, as $n \rightarrow \infty$, all nodes are correctly clustered with high probability. Moreover, we theoretically demonstrate that for finite samples, two-step Refined TCSC can substantially accelerate the convergence rate of the clustering error. Third, we propose a data-driven method for selecting the number of communities K under the PABM, which outperforms the loss-plus-penalty approach proposed by [Noroozi et al. \(2021b\)](#) in simulations.

The rest of this paper is organized as follows. [Section 2](#) introduces the PABM framework. [Section 3](#) studies the eigenspace properties and presents our proposed algorithms TCSC and R-TCSC. In [Section 4](#), we establish upper bounds on the clustering error rates for both algorithms. [Section 5](#) presents simulation studies demonstrating the numerical properties of TCSC and R-TCSC. [Section 6](#) addresses the selection of the number of communities when it is unknown. [Section 7](#) shows the practical utility of our methods through applications to two real-world datasets. [Section 8](#) includes a few concluding remarks.

2 Preliminaries

We begin by introducing useful notations. Let $[n] \doteq \{1, \dots, n\}$ for any $n \in \mathbb{N}_+$, and $|\mathcal{S}|$ be the cardinality of a set \mathcal{S} . Throughout the paper, we use C to denote generic constants whose values may vary from line to line. For positive sequences $\{x_n\}_{n=1}^\infty$ and $\{y_n\}_{n=1}^\infty$, $x_n \gtrsim y_n$ means that $x_n \geq Cy_n$ for some $C > 0$; $x_n \lesssim y_n$ means that $x_n \leq Cy_n$ for some

$C > 0$; $x_n \asymp y_n$ means that $\frac{1}{C}y_n \leq x_n \leq Cy_n$ for some $C \geq 1$; $x_n \gg y_n$ means that $y_n = o(x_n)$; $x_n \ll y_n$ means $x_n = o(y_n)$. For $\mathbf{x} = (x_1, \dots, x_n)^\top \in \mathbb{R}^n$, $\|\mathbf{x}\| = \sqrt{\sum_{i=1}^n x_i^2}$. For $\mathbf{M} = (M_{ij})_{m \times n} \in \mathbb{R}^{m \times n}$, let $\|\mathbf{M}\|_F = \sqrt{\sum_{i=1}^m \sum_{j=1}^n M_{ij}^2}$, $\sigma_r(\mathbf{M})$ denote the r -th largest singular value of \mathbf{M} and $\|\mathbf{M}\|_{\text{op}} = \sigma_1(\mathbf{M})$, where $1 \leq r \leq \min\{m, n\}$. For a square matrix \mathbf{M} , $\text{diag}(\mathbf{M})$ denotes the diagonal matrix whose diagonal entries are those of \mathbf{M} .

We consider the undirected network $G = (V, E)$ with the node set $V = [n]$, the edge set $E \subseteq \{(i, j) : i, j \in V\}$, and the adjacency matrix $\mathbf{A} = (A_{ij})_{n \times n} \in \{0, 1\}^{n \times n}$. Here, $A_{ij} = 1$ if $(i, j) \in E$, otherwise $A_{ij} = 0$. Suppose that there is no self-loop in network G , i.e., $A_{ii} = 0$ for each node $i \in V$. As in [Sengupta and Chen \(2017\)](#) and [Noroozi et al. \(2021b\)](#), the network G can be characterized by the Popularity Adjusted Block Model (PABM):

$$A_{ij} = A_{ji} \stackrel{\text{ind}}{\sim} \text{Bern}(\theta_{ij}) \text{ for all } i < j \in [n], \quad \text{and} \quad A_{ii} \equiv 0 \text{ for all } i \in [n], \quad (1)$$

where $\theta_{ij} = \lambda_{i\mathbf{c}^*(j)} \lambda_{j\mathbf{c}^*(i)}$, $\boldsymbol{\Lambda} = (\lambda_{ik})_{n \times K} \in [0, 1]^{n \times K}$ and $\mathbf{c}^* = (\mathbf{c}^*(1), \dots, \mathbf{c}^*(n))^\top \in [K]^n$ is the community label. Let $\boldsymbol{\Theta} = (\theta_{ij})_{n \times n}$. And we have that $\mathbb{E}\mathbf{A} = \boldsymbol{\Theta} - \text{diag}(\boldsymbol{\Theta})$.

Our objective is to recover the true community labels \mathbf{c}^* . Following [Sengupta and Chen \(2017\)](#) and [Noroozi et al. \(2021b\)](#), we are concerned only with the partition structure and not the specific label assignments. Accordingly, for any true label vector $\mathbf{c}^* \in [K]^n$, we evaluate an estimator $\hat{\mathbf{c}} \in [K]^n$ using the following loss function:

$$\ell(\mathbf{c}^*, \hat{\mathbf{c}}) = \min_{\pi: [K] \rightarrow [K]} \frac{1}{n} \sum_{i=1}^n \mathbb{I}\{\mathbf{c}^*(i) \neq \pi(\hat{\mathbf{c}}(i))\}. \quad (2)$$

Let $\pi^*(\cdot)$ be the optimal permutation achieving the minimum in (2), which means $n \ell(\mathbf{c}^*, \hat{\mathbf{c}}) = \sum_{i=1}^n \mathbb{I}\{\mathbf{c}^*(i) \neq \pi^*(\hat{\mathbf{c}}(i))\}$. For the sake of notational simplicity, we replace $\pi^*[\hat{\mathbf{c}}]$ by $\hat{\mathbf{c}}$ later, where $\pi^*[\hat{\mathbf{c}}] = (\pi^*(\hat{\mathbf{c}}(1)), \dots, \pi^*(\hat{\mathbf{c}}(n)))^\top$.

[Sengupta and Chen \(2017\)](#) introduced the PABM likelihood modularity approach to estimate community labels by maximizing the likelihood function. [Noroozi et al. \(2021a,b\)](#) leveraged a key structural property of the PABM that $\boldsymbol{\theta}_i$ can and only can be expressed by $\{\boldsymbol{\theta}_j\}_{j: \mathbf{c}^*(j) = \mathbf{c}^*(i)}$ to apply the sparse subspace clustering (SSC) directly to the adjacency matrix \mathbf{A} to estimate the community label vector \mathbf{c}^* , where $\boldsymbol{\theta}_i$ is the i -th row of $\boldsymbol{\Theta}$. In contrast, [Koo et al. \(2023\)](#) recovered the community label vector \mathbf{c}^* using the relationship

between the eigenspace of Θ and community labels \mathbf{c}^* . Instead of applying SSC to \mathbf{A} as in [Noroozi et al. \(2021b\)](#), they applied the SSC to the spectral embedding of \mathbf{A} .

3 Methodology

This section aims to implement spectral clustering under the PABM. Subsection 3.1 examines the eigenspace properties of the edge probability matrix and explores its relationship with the underlying community structure. Building on these insights, we present the proposed TCSC algorithm in Subsection 3.2 and R-TCSC algorithm in Subsection 3.3.

3.1 Structural Properties of the PABM

The foundation of spectral clustering algorithms lies in analyzing the relationship between the eigenvectors of the adjacency matrix \mathbf{A} with those of the edge probability matrix Θ , and in understanding how the eigenstructure of Θ relates to the true community labels \mathbf{c}^* . For example, under mild conditions, [Lei and Rinaldo \(2015\)](#) showed that, in the SBM, the eigenvector matrix Ξ_{SBM} of the edge probability matrix Θ_{SBM} satisfies that two nodes belong to the same community if and only if their corresponding rows in Ξ_{SBM} are identical. Similarly, in the DCSBM, the eigenvector matrix Ξ_{DCSBM} of the edge probability matrix Θ_{DCSBM} satisfies that two nodes belong to the same community if and only if their corresponding rows in Ξ_{DCSBM} are proportional.

To implement spectral clustering under the PABM, we start with a spectral analysis of the edge probability matrix Θ . As noted in [Noroozi et al. \(2021b\)](#), by permuting the nodes, Θ can be rearranged into a block matrix consisting of K^2 rank-one submatrices:

$$\Theta = \begin{bmatrix} \boldsymbol{\lambda}^{(1,1)} \boldsymbol{\lambda}^{(1,1)\top} & \dots & \boldsymbol{\lambda}^{(1,K)} \boldsymbol{\lambda}^{(K,1)\top} \\ \vdots & & \vdots \\ \boldsymbol{\lambda}^{(K,1)} \boldsymbol{\lambda}^{(1,K)\top} & \dots & \boldsymbol{\lambda}^{(K,K)} \boldsymbol{\lambda}^{(K,K)\top} \end{bmatrix}, \quad (3)$$

where $\boldsymbol{\lambda}^{(k,l)} = (\lambda_{il})_{i:\mathbf{c}^*(i)=k} \in [0, 1]^{n_k(\mathbf{c}^*) \times 1}$ for each $k, l \in [K]$, with $n_k(\mathbf{c}) = \sum_{i=1}^n \mathbb{I}\{\mathbf{c}(i) = k\}$ for any general $\mathbf{c} \in [K]^n$. To avoid degeneracy in the model parameters, we suppose that

Θ has rank K^2 . This is equivalent to Assumption A1* in Noroozi et al. (2021b), which requires that $\lambda^{(k,1)}, \dots, \lambda^{(k,K)}$ are linearly independent for each $k \in [K]$.

In the PABM, let $\Xi D \Xi^\top$ be an eigenvalue decomposition of Θ , where $\Xi = [\xi_1, \dots, \xi_n]^\top$. Among existing works on the PABM, only Koo et al. (2023) further analyzed the structure of Ξ . Specifically, their Theorem 2 states that, when $\lambda_{i\mathbf{c}^*(i)} > 0$ for all $i \in [n]$, then $\xi_i^\top \xi_j = 0$ if and only if $\mathbf{c}^*(i) \neq \mathbf{c}^*(j)$. The logic of their algorithms and theoretical developments relies entirely on this argument. However, we provide Example 1 to highlight issues in the statement and proof of their Theorem 2. Notably, their proof only establishes that $\xi_i^\top \xi_j = 0$ if $\mathbf{c}^*(i) \neq \mathbf{c}^*(j)$, but does not prove the converse that orthogonality necessarily implies different community memberships (i.e., $\xi_i^\top \xi_j = 0$ leads to $\mathbf{c}^*(i) \neq \mathbf{c}^*(j)$). In fact, when $\lambda_{i\mathbf{c}^*(i)} > 0$ for each $i \in [n]$, we will provide a simple example in Example 1 to show that there can be many instances where $\xi_i^\top \xi_j = 0$ despite $\mathbf{c}^*(i) = \mathbf{c}^*(j)$; that is, the eigenvectors corresponding to nodes within the same community can still be orthogonal.

Example 1. Set $n = 8$, $K = 2$, $\Lambda = \frac{1}{4} \begin{bmatrix} 2 & 2 & 2 & 2 & 1 & 1 & 2 & 2 \\ 2 & 2 & 1 & 1 & 4 & 4 & 4 & 4 \end{bmatrix}^\top$ and $\mathbf{c}^* = (1, 1, 1, 1, 2, 2, 2, 2)^\top$. Let $\mathbf{1}_2$ be an 2-dimensional vector whose elements are all 1. Then, we have

$$(\xi_i^\top \xi_j)_{i,j \in [8]} = \frac{1}{2} \begin{bmatrix} \mathbf{1}_2 \mathbf{1}_2^\top & \mathbf{0}_{2 \times 2} & \mathbf{0}_{2 \times 2} & \mathbf{0}_{2 \times 2} \\ \mathbf{0}_{2 \times 2} & \mathbf{1}_2 \mathbf{1}_2^\top & \mathbf{0}_{2 \times 2} & \mathbf{0}_{2 \times 2} \\ \mathbf{0}_{2 \times 2} & \mathbf{0}_{2 \times 2} & \mathbf{1}_2 \mathbf{1}_2^\top & \mathbf{0}_{2 \times 2} \\ \mathbf{0}_{2 \times 2} & \mathbf{0}_{2 \times 2} & \mathbf{0}_{2 \times 2} & \mathbf{1}_2 \mathbf{1}_2^\top \end{bmatrix}.$$

Note that $\xi_1^\top \xi_3 = \xi_1^\top \xi_4 = \xi_2^\top \xi_3 = \xi_2^\top \xi_4 = 0$ even though $\mathbf{c}^*(1) = \mathbf{c}^*(2) = \mathbf{c}^*(3) = \mathbf{c}^*(4) = 1$, which implies that $\xi_i^\top \xi_j > 0$ may not hold even if $\mathbf{c}^*(i) = \mathbf{c}^*(j)$.

The absence of a comprehensive and rigorous spectral analysis of Ξ in the PABM has hindered the development of effective spectral clustering algorithms. To address this gap, we present the following proposition, which establishes explicit relationships between the eigenspace Ξ of the edge probability matrix Θ and the true community labels \mathbf{c}^* .

Proposition 1. Suppose that the rank of Θ is K^2 , and let $\Xi = (\xi_{iu})_{n \times K^2}$ be the eigenvector matrix of Θ corresponding to the K^2 nonzero eigenvalues. Let $\Xi^{(k)} = (\xi_{iu})_{i:\mathbf{c}^*(i)=k, u \in [K^2]}$

and $\mathbf{\Lambda}^{(k,\cdot)} = (\lambda_{il})_{i:\mathbf{c}^*(i)=k, l \in [K]}$. Then, for each $k \in [K]$, we have

$$\mathbf{\Xi}^{(k)} = \mathbf{\Lambda}^{(k,\cdot)} \mathbf{Z}_k, \quad (4)$$

where $\mathbf{Z}_k \in \mathbf{R}^{K \times K^2}$ satisfies that $\mathbf{Z}_k \mathbf{Z}_l^\top = \mathbf{0}_{K \times K}$ for each $l \neq k$ and $\mathbf{Z}_k \mathbf{Z}_k^\top = (\mathbf{\Lambda}^{(k,\cdot)\top} \mathbf{\Lambda}^{(k,\cdot)})^{-1}$.

Proposition 1 shows that each row of the eigenvector matrix $\mathbf{\Xi}$ satisfies $\boldsymbol{\xi}_i^\top = \boldsymbol{\lambda}_i^\top \mathbf{Z}_{\mathbf{c}^*(i)}$, where $\boldsymbol{\lambda}_i$ is the i -th row of $\mathbf{\Lambda} \in [0, 1]^{n \times K}$. This structure underscores the inadequacy of directly applying K-means clustering to the rows of $\mathbf{\Xi}$, as also noted in Noroozi et al. (2021b). Specifically, the Euclidean distance $\|\boldsymbol{\xi}_i - \boldsymbol{\xi}_j\|$ depends not only on the community labels $\mathbf{c}^*(i)$ and $\mathbf{c}^*(j)$, but also on the latent node-specific vectors $\boldsymbol{\lambda}_i$ and $\boldsymbol{\lambda}_j$.

More importantly, Proposition 1 also implies that $\boldsymbol{\xi}_i^\top \boldsymbol{\xi}_j = 0$ as long as $\mathbf{c}^*(i) \neq \mathbf{c}^*(j)$. This motivates a different perspective based on angular similarity. Specifically, for each $i, j \in [n]$ we define the angle-based similarity between nodes i and j as

$$\tau_{ij} = |\cos(\boldsymbol{\xi}_i, \boldsymbol{\xi}_j)|.$$

Although τ_{ij} is defined in terms of the eigenvector matrix $\mathbf{\Xi}$, our analysis will reveal an explicit relationship between $\mathbf{\Xi}$, the parameter matrix $\mathbf{\Lambda}$, and the true labels \mathbf{c}^* .

For each $k \in [K]$, define $\mathbf{P}_k = \mathbf{Z}_k \mathbf{Z}_k^\top = (\mathbf{\Lambda}^{(k,\cdot)\top} \mathbf{\Lambda}^{(k,\cdot)})^{-1}$, and $D_{\mathbf{P}_k}(\boldsymbol{\lambda}_i, \boldsymbol{\lambda}_j) = \boldsymbol{\lambda}_i^\top \mathbf{P}_k \boldsymbol{\lambda}_j$. Using Proposition 1, we directly obtain Corollary 1, which characterizes the relationship between the angle similarity τ_{ij} and the underlying parameters $\mathbf{\Lambda}$, $\mathbf{c}^*(i)$, and $\mathbf{c}^*(j)$. This connection clarifies the assumptions for our theoretical guarantees and guides the development of subsequent results.

Corollary 1. *Under the same conditions of Proposition 1, for $i, j \in [n]$, we have*

$$\tau_{ij} = \begin{cases} \left| \frac{D_{\mathbf{P}_{\mathbf{c}^*(i)}}(\boldsymbol{\lambda}_i, \boldsymbol{\lambda}_j)}{D_{\mathbf{P}_{\mathbf{c}^*(i)}}^{1/2}(\boldsymbol{\lambda}_i, \boldsymbol{\lambda}_i) D_{\mathbf{P}_{\mathbf{c}^*(i)}}^{1/2}(\boldsymbol{\lambda}_j, \boldsymbol{\lambda}_j)} \right|, & \mathbf{c}^*(i) = \mathbf{c}^*(j); \\ 0, & \mathbf{c}^*(i) \neq \mathbf{c}^*(j). \end{cases}$$

3.2 Thresholded Cosine Spectral Clustering (TCSC)

To implement spectral clustering under the PABM, we begin by estimating the angle-based similarity measures $(\tau_{ij})_{i,j \in [n]}$. Specifically, we compute the eigenvectors of the adjacency

matrix \mathbf{A} , and construct the matrix $\hat{\mathbf{\Xi}}$ by selecting the eigenvectors corresponding to the K^2 largest eigenvalues in absolute value. For each $i, j \in [n]$, we estimate τ_{ij} as

$$\hat{\tau}_{ij} = \left| \cos \left(\hat{\boldsymbol{\xi}}_{i\cdot}, \hat{\boldsymbol{\xi}}_{j\cdot} \right) \right|,$$

where $\hat{\boldsymbol{\xi}}_i$ denotes the i -th row of $\hat{\mathbf{\Xi}}$. We then define $\hat{\boldsymbol{\tau}}_i = (\hat{\tau}_{i1}, \dots, \hat{\tau}_{in})^\top$ for node i .

However, applying K-means clustering to $\{\hat{\boldsymbol{\tau}}_i\}_{i \in [n]}$ cannot effectively identify the underlying communities. To illustrate this issue, we provide Example 2 below to show that, although node 8 belongs to the second community, $\boldsymbol{\tau}_8$ is closer to the center of the first community, even using the true similarity measures $\{\boldsymbol{\tau}_i\}_{i \in [n]}$, as shown in Table 1.

Example 2. Set $n = 8$, $K = 2$, $\mathbf{\Lambda} = \frac{1}{10} \begin{bmatrix} 1 & 10 & 10 & 8 & 1 & 8 & 6 & 10 \\ 2 & 8 & 8 & 10 & 2 & 10 & 8 & 8 \end{bmatrix}^\top$, and $\mathbf{c}^* = (1, 1, 1, 1, 2, 2, 2, 2)^\top$. Let $\bar{\boldsymbol{\tau}}_k = \frac{1}{4} \sum_{i: \mathbf{c}^*(i)=k} \boldsymbol{\tau}_i$ for $k \in [2]$. Then, we can compute the distance from $\boldsymbol{\tau}_i$, for each $i \in [8]$, to community centers $\bar{\boldsymbol{\tau}}_1$ and $\bar{\boldsymbol{\tau}}_2$ in the following table.

Table 1: The distance to two community centers $\bar{\boldsymbol{\tau}}_1$ and $\bar{\boldsymbol{\tau}}_2$.

i	1	2	3	4	5	6	7	8
$\ \boldsymbol{\tau}_i - \bar{\boldsymbol{\tau}}_1\ ^2$	1.76	1.28	1.28	0.93	3.43	3.37	3.51	1.99
$\ \boldsymbol{\tau}_i - \bar{\boldsymbol{\tau}}_2\ ^2$	3.43	3.45	3.45	3.23	0.65	0.22	0.31	2.81

To address this issue, we define the thresholded cosine measures $\tilde{\boldsymbol{\tau}}_i = (\tilde{\tau}_{ij}, \dots, \tilde{\tau}_{in})^\top$ with $\tilde{\tau}_{ij} = \mathbb{I}\{\hat{\tau}_{ij} \geq d_n\}$ for each $i \in [n]$. This thresholding step is motivated by the observation that, for most node pairs (i, j) within the same community, $\boldsymbol{\xi}_{i\cdot}$ and $\boldsymbol{\xi}_{j\cdot}$ are not orthogonal, and their true similarity τ_{ij} does not decay rapidly toward zero. To formalize this idea, we define $\mathcal{G}_i = \{j \in [n] : \mathbf{c}^*(j) = \mathbf{c}^*(i), |\tau_{ij}| \geq \phi_{1,n}\}$ for each $i \in [n]$, where \mathbf{c}^* denotes the true community assignment, and $\phi_{1,n} \in (0, 1]$ is a sequence bounded away from zero. We assume that there exists a sequence $\phi_{1,n}$ sufficiently large to be robust to noise, such that $|\mathcal{G}_i| = n_{\mathbf{c}^*(i)}(\mathbf{c}^*)(1 - o(1))$, where $n_{\mathbf{c}^*(i)}(\mathbf{c}^*)$ denotes the size of community $\mathbf{c}^*(i)$. Given this, we set the threshold as $d_n = \phi_{1,n}/2$, which ensures the following desirable properties: for all $i \in [n]$ and all j such that $\mathbf{c}^*(j) \neq \mathbf{c}^*(i)$, we have $\tilde{\tau}_{ij} = 0$; and for all $j \in \mathcal{G}_i$, we have

$\tilde{\tau}_{ij} = 1$. Consequently, $\tilde{\boldsymbol{\tau}}_i$ closely approximates the vector $\mathbf{a}_{\mathbf{c}^*(i)}$, where for each $k \in [K]$, $\mathbf{a}_k = (a_k(1), \dots, a_k(n))^\top$ with $a_k(i) = 1$ if $\mathbf{c}^*(i) = k$ and $a_k(i) = 0$ otherwise.

After obtaining $(\tilde{\boldsymbol{\tau}}_i)_{i \in [n]}$, we apply K-means clustering to recover the community labels \mathbf{c}^* . It is known that finding the global optimum for the K -means clustering problem is NP-hard. Thus, we employ an approximation algorithm that computes a $(1 + \varepsilon)$ -approximate solution in polynomial time, for any fixed constant $\varepsilon > 0$. Such algorithms have been studied and theoretically justified in [Kumar et al. \(2004\)](#) and [Lei and Rinaldo \(2015\)](#). Specifically, we solve the following $(1 + \varepsilon)$ -approximate K -means optimization problem to find some $\hat{\mathbf{c}}^{(0)} = (\hat{\mathbf{c}}^{(0)}(1), \dots, \hat{\mathbf{c}}^{(0)}(n))^\top \in [K]^n$, such that

$$\sum_{k=1}^K \min_{\tilde{\boldsymbol{\nu}}_k \in \mathbb{R}^n} \sum_{i: \hat{\mathbf{c}}^{(0)}(i)=k} \|\tilde{\boldsymbol{\tau}}_i - \tilde{\boldsymbol{\nu}}_k\|^2 \leq (1 + \varepsilon) \min_{\tilde{\mathbf{c}} \in [K]^n} \sum_{k=1}^K \min_{\tilde{\boldsymbol{\nu}}_k \in \mathbb{R}^n} \sum_{i: \tilde{\mathbf{c}}(i)=k} \|\tilde{\boldsymbol{\tau}}_i - \tilde{\boldsymbol{\nu}}_k\|^2. \quad (5)$$

These three steps are integrated into the proposed Thresholded Cosine Spectral Clustering (TCSC), which is summarized in the following Algorithm 1.

Algorithm 1 Thresholded Cosine Spectral Clustering (TCSC)

Input: Adjacency matrix \mathbf{A} , and the number of communities $K \geq 2$.

Output: An estimator $\hat{\mathbf{c}}^{(0)} \in [K]^n$ of the community label vector $\mathbf{c}^* \in [K]^n$.

- 1: Estimate the angle-based similarity measures via $(\hat{\tau}_{ij})_{i,j \in [n]}$ with $\hat{\tau}_{ij} = \left| \cos \left(\hat{\boldsymbol{\xi}}_i, \hat{\boldsymbol{\xi}}_j \right) \right|$.
 - 2: For $i \in [n]$, solve the thresholded measure $\tilde{\boldsymbol{\tau}}_i = (\tilde{\tau}_{ij}, \dots, \tilde{\tau}_{in})^\top$ with $\tilde{\tau}_{ij} = \mathbb{I}\{\hat{\tau}_{ij} \geq d_n\}$.
 - 3: For $\varepsilon > 0$, solve $\hat{\mathbf{c}}^{(0)}$ from the $(1 + \varepsilon)$ -approximation K -means problem (5).
-

Figure 1 provides an intuitive overview of Algorithm 1. When the signal-to-noise ratio is sufficiently high, the vectors $\hat{\boldsymbol{\xi}}_i$ and $\hat{\boldsymbol{\xi}}_j$ corresponding to nodes from different communities are nearly orthogonal, as illustrated in Figure 1(a). We then compute the estimated angular similarity $\hat{\tau}_{ij}$ to capture the similarity between node pairs (i, j) . However, as shown in Example 2, even in the noiseless population case, it is generally impossible to directly perform K -means clustering on the vectors $\{\boldsymbol{\tau}_i\}_{i \in [n]}$. To overcome this, we apply a thresholding step to $\hat{\boldsymbol{\tau}}_i$, resulting in the vectors $\tilde{\boldsymbol{\tau}}_i$, which concentrate around the idealized community centers $\mathbf{a}_{\mathbf{c}^*(i)}$, as shown in Figure 1(c). This concentration effect justifies applying K -means clustering to the thresholded vectors $\tilde{\boldsymbol{\tau}}_i$.

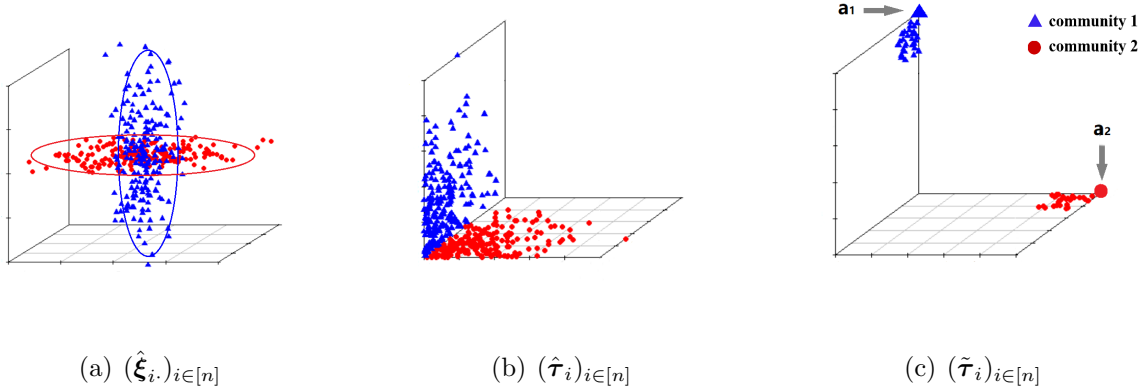


Figure 1: Conceptual Figure. An illustration of Algorithm 1 for $K = 2$. The red circles and blue triangles represent nodes from two different communities. Although $\hat{\xi}_i$, $\hat{\tau}_i$ and $\tilde{\tau}_i$ lie in high-dimensional spaces, this figure provides a low-dimensional visualization for intuitive understanding only.

3.3 Refined Thresholded Cosine Spectral Clustering (R-TCSC)

The TCSC provides an effective implementation under the PABM and yields a weakly consistent estimator, as shown in Section 4. However, under mild conditions, it does not guarantee exact recovery. To improve estimation accuracy and achieve strong consistency, we incorporate a refinement step to enhance the accuracy of community label estimation.

Refinements are commonly used to improve initial estimators and have proven effective across various network models. Gao et al. (2017); Yun and Proutiere (2016); Gao et al. (2018); Xu et al. (2020) employed refinement techniques in the Stochastic Block Model (SBM), Labeled SBM, Degree-Corrected SBM, and Weighted SBM, respectively. The refinement step can be viewed as a node-wise classification task: for each node, its community label is updated by treating the labels of the remaining $n - 1$ nodes as known. Different refinement strategies vary in how they measure similarity between the target node and the K communities. Likelihood-based similarity measures are commonly used in prior works such as Gao et al. (2017); Yun and Proutiere (2016); Xu et al. (2020). Due to the complexity of DCSBM, which requires estimating $n + K^2$ parameters in addition to the community labels, Gao et al. (2018) instead adopted a simpler approach based on edge frequencies.

However, for the more flexible and complex PABM, neither likelihood-based nor edge frequency-based similarity measures are suitable. This is because the PABM involves nK parameters, exceeding those in the DCSBM, yet it does not impose higher within-community edge densities. Consequently, achieving exact recovery of community labels through refinement under reasonable conditions presents two key challenges: (1) developing a refinement strategy with a similarity measure tailored to the PABM; and (2) determining whether such a refinement can upgrade a weakly consistent initializer to strong consistency.

To address these challenges, we first propose an angle-based similarity measure tailored to the structure of the PABM. We then show in Theorem 2 that this measure enables exact recovery of the true community labels \mathbf{c}^* with high probability through a one-step refinement step. Specially, suppose for each $i, j \in [n]$ and $k \in [K]$, we have $\lambda_{ik}, \lambda_{jk} \neq 0$, and the set of vectors $\{\boldsymbol{\lambda}^{(k,l)}\}_{l \in [K]}$ is linearly independent, where $\boldsymbol{\lambda}^{(k,l)} = (\lambda_{il})_{i:\mathbf{c}^*(i)=k}$. Under these conditions, it can be shown that $\cos(\boldsymbol{\theta}_{i\cdot}^{(l)}, \boldsymbol{\theta}_{j\cdot}^{(l)}) = \cos(\lambda_{il}\boldsymbol{\lambda}^{(l,\mathbf{c}^*(i))}, \lambda_{jl}\boldsymbol{\lambda}^{(l,\mathbf{c}^*(j))})$ equals 1 if $\mathbf{c}^*(i) = \mathbf{c}^*(j)$ and less than 1 if $\mathbf{c}^*(i) \neq \mathbf{c}^*(j)$. Let $\boldsymbol{\theta}_{i\cdot}^{(l)} = (\theta_{ij})_{j:\mathbf{c}^*(j)=l}$ be the edge probability vector between node i and nodes in community l . Define $\bar{\boldsymbol{\theta}}^{(k,l)} = \sum_{v:\mathbf{c}^*(v)=k} \boldsymbol{\theta}_{v\cdot}^{(l)} / n_k(\mathbf{c}^*)$ for each $k \in [K]$. We have that $\cos(\boldsymbol{\theta}_{i\cdot}^{(l)}, \bar{\boldsymbol{\theta}}^{(k,l)}) = \cos(\lambda_{il}\boldsymbol{\lambda}^{(l,\mathbf{c}^*(i))}, \frac{1}{n_k(\mathbf{c}^*)} \mathbf{1}_{n_k(\mathbf{c}^*)}^\top \boldsymbol{\lambda}^{(k,l)} \boldsymbol{\lambda}^{(l,k)})$ equals 1 if $\mathbf{c}^*(i) = k$ and less than 1 if $\mathbf{c}^*(i) \neq k$, where $\mathbf{1}_m$, $m \in \mathbb{N}_+$, denotes a vector whose elements are all 1. If the community labels of all nodes except i are known and denoted \mathbf{c}_{-i}^* , the label $\mathbf{c}^*(i)$ can be recovered by solving

$$\arg \max_{k \in [K]} \sum_{l=1}^K \cos(\boldsymbol{\theta}_{i\cdot}^{(l)}, \bar{\boldsymbol{\theta}}^{(k,l)}). \quad (6)$$

The population-level insights motivate refining community assignments by maximizing the aggregated inter-cluster cosine similarity between each node and the estimated community centers, using the initial label estimate $\hat{\mathbf{c}}^{(0)} = (\hat{\mathbf{c}}^{(0)}(1), \dots, \hat{\mathbf{c}}^{(0)}(n))^\top$ obtained from Algorithm 1.

Based on $\hat{\mathbf{c}}^{(0)}$, we estimate $\boldsymbol{\theta}_{i\cdot}^{(l)} = (\theta_{ij})_{j:\mathbf{c}^*(j)=l}$ by $\mathbf{A}_{i\cdot}^{(l)}(\hat{\mathbf{c}}^{(0)}) = (A_{ij})_{j:\hat{\mathbf{c}}^{(0)}(j)=l}$, and estimate $\bar{\boldsymbol{\theta}}^{(k,l)} = \sum_{v:\mathbf{c}^*(v)=k} \boldsymbol{\theta}_{v\cdot}^{(l)} / n_k(\mathbf{c}^*)$ by $\bar{\mathbf{A}}^{(k,l)}(\hat{\mathbf{c}}^{(0)}) = \sum_{v:\hat{\mathbf{c}}^{(0)}(v)=k} \mathbf{A}_{v\cdot}^{(l)}(\hat{\mathbf{c}}^{(0)}) / n_k(\hat{\mathbf{c}}^{(0)})$, replacing $\boldsymbol{\Theta}$ with \mathbf{A} and \mathbf{c}^* with $\hat{\mathbf{c}}^{(0)}$. Each node i updates its community label by solving:

$$\hat{\mathbf{c}}^{(1)}(i) = \arg \max_{k \in [K]} \sum_{l=1}^K \frac{\mathbf{A}_{i\cdot}^{(l)}(\hat{\mathbf{c}}^{(0)})^\top \bar{\mathbf{A}}^{(k,l)}(\hat{\mathbf{c}}^{(0)})}{\|\mathbf{A}_{i\cdot}^{(l)}(\hat{\mathbf{c}}^{(0)})\| \|\bar{\mathbf{A}}^{(k,l)}(\hat{\mathbf{c}}^{(0)})\|}. \quad (7)$$

Applying this update to all nodes yields the one-step refined estimate $\hat{\mathbf{c}}^{(1)}$.

Before proceeding, we introduce the leave-one-out version $\bar{\mathbf{A}}_{-i}^{(k,l)}(\hat{\mathbf{c}}^{(0)})$, a modification of $\bar{\mathbf{A}}^{(k,l)}(\hat{\mathbf{c}}^{(0)})$ that excludes the contribution from node i . It is formally defined as $\bar{\mathbf{A}}_{-i}^{(k,l)}(\hat{\mathbf{c}}^{(0)}) = n_k^{-1}(\hat{\mathbf{c}}^{(0)}) \sum_{j \in [n]} \mathbf{A}_{j \cdot}^{(l)}(\hat{\mathbf{c}}^{(0)}) \mathbb{I}\{\hat{\mathbf{c}}^{(0)}(j) = k, j \neq i\}$. This construction ensures that, $\bar{\mathbf{A}}_{-i}^{(k,l)}(\tilde{\mathbf{c}})$ is independent of $\mathbf{A}_{i \cdot}^{(l)}(\tilde{\mathbf{c}})$ for any fixed $\tilde{\mathbf{c}} \in [K]^n$, thereby simplifying the theoretical analysis. Thus, the refinement update is modified as:

$$\hat{\mathbf{c}}^{(1)}(i) = \operatorname{argmax}_{k \in [K]} \sum_{l=1}^K \frac{\mathbf{A}_{i \cdot}^{(l)}(\hat{\mathbf{c}}^{(0)})^\top \bar{\mathbf{A}}_{-i}^{(k,l)}(\hat{\mathbf{c}}^{(0)})}{\|\mathbf{A}_{i \cdot}^{(l)}(\hat{\mathbf{c}}^{(0)})\| \|\bar{\mathbf{A}}_{-i}^{(k,l)}(\hat{\mathbf{c}}^{(0)})\|}. \quad (8)$$

Integrating both initialization and refinement steps, the proposed One-step Refined Thresholded Cosine Spectral Clustering (R-TCSC) Algorithm is presented as Algorithm 2.

Algorithm 2 The One-Step Refined Thresholded Cosine Spectral Clustering (R-TCSC)

Input: Adjacency matrix \mathbf{A} , number of communities $K \geq 2$.

Output: A refined estimator $\hat{\mathbf{c}} := \hat{\mathbf{c}}^{(1)} \in [K]^n$ of the community label vector $\mathbf{c}^* \in [K]^n$.

- 1: Apply Algorithm 1 to obtain the initial label vector $\hat{\mathbf{c}}^{(0)}$.
- 2: For each $i \in [n]$, update each $\hat{\mathbf{c}}^{(1)}(i)$ by maximizing the cosine similarity:

$$\hat{\mathbf{c}}^{(1)}(i) = \operatorname{argmax}_{k \in [K]} \sum_{l=1}^K \frac{\mathbf{A}_{i \cdot}^{(l)}(\hat{\mathbf{c}}^{(0)})^\top \bar{\mathbf{A}}_{-i}^{(k,l)}(\hat{\mathbf{c}}^{(0)})}{\|\mathbf{A}_{i \cdot}^{(l)}(\hat{\mathbf{c}}^{(0)})\| \|\bar{\mathbf{A}}_{-i}^{(k,l)}(\hat{\mathbf{c}}^{(0)})\|}. \quad (9)$$

Figure 2 illustrates the refinement process in Algorithm 2 for a network with 512 nodes. The one-step R-TCSC improves the initial estimate and successfully corrects all 6 initially misclustered nodes. We define the similarity score between node i and community k as $S_{\cos,ik}(\hat{\mathbf{c}}^{(0)}) = \sum_{l \in [K]} \cos(\mathbf{A}_{i \cdot}^{(l)}(\hat{\mathbf{c}}^{(0)}), \bar{\mathbf{A}}_{-i}^{(k,l)}(\hat{\mathbf{c}}^{(0)}))$, leading to the update $\hat{\mathbf{c}}^{(1)}(i) = \operatorname{argmax}_{k \in [K]} S_{\cos,ik}(\hat{\mathbf{c}}^{(0)})$. Let $\mathbf{S}_{\cos}(\hat{\mathbf{c}}^{(1)}) = (S_{\cos,ik}(\hat{\mathbf{c}}^{(1)}))_{i \in [n], k \in [K]}$, with columns $\mathbf{S}_{\cos}(\hat{\mathbf{c}}^{(1)})[:, 1]$, $\mathbf{S}_{\cos}(\hat{\mathbf{c}}^{(1)})[:, 2]$ representing similarity scores to each community. The diagonal line of Figure 2 serves as the decision boundary between communities. Figures 2(a) and 2(b) show that all misclustered nodes (120, 155, 278, 318, 417 and 495) are correctly clustered after the one-step refinement.

Extensive numerical studies (see Section 5.2) confirm that when n is sufficiently large (e.g., $n = 2^{10}$), the one-step refinement $\hat{\mathbf{c}}^{(1)}$ reliably recovers the true community labels,

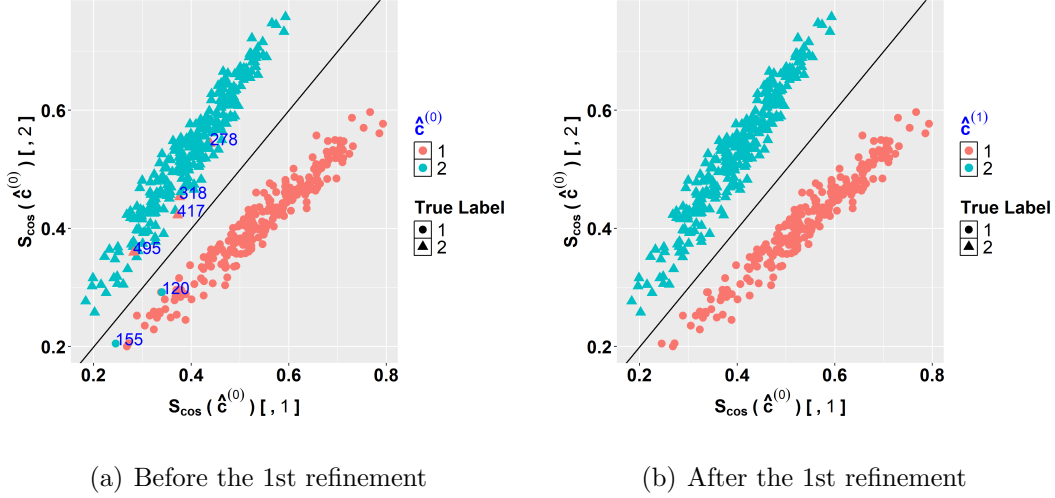


Figure 2: An illustration of the one-step refinement for a network of 512 nodes with $K = 2$ and incorrectly estimated node numbers marked in each plot.

aligned with the strong consistency result established for Algorithm 2 in Theorem 2.

Algorithm 3 Two-Step Refined Thresholded Cosine Spectral Clustering (R-TCSC)

Input: Adjacency matrix \mathbf{A} , number of communities $K \geq 2$.

Output: A refined estimator $\hat{\mathbf{c}} := \hat{\mathbf{c}}^{(2)} \in [K]^n$ of the community label vector $\mathbf{c}^* \in [K]^n$.

- 1: Apply Algorithm 2 to obtain the estimated label vector $\hat{\mathbf{c}}^{(0)}$ via one-step refinement.
- 2: For each $i \in [n]$, update each $\hat{\mathbf{c}}^{(2)}(i)$ by maximizing the cosine similarity:

$$\hat{\mathbf{c}}^{(2)}(i) = \operatorname{argmax}_{k \in [K]} \sum_{l=1}^K \frac{\mathbf{A}_{i \cdot}^{(l)}(\hat{\mathbf{c}}^{(1)})^\top \bar{\mathbf{A}}_{-i}^{(k,l)}(\hat{\mathbf{c}}^{(1)})}{\|\mathbf{A}_{i \cdot}^{(l)}(\hat{\mathbf{c}}^{(1)})\| \|\bar{\mathbf{A}}^{(k,l)}(\hat{\mathbf{c}}^{(1)})\|}. \quad (10)$$

However, when the sample size is relatively small (e.g., $n = 2^7$ or 2^8), applying an additional refinement step (i.e., two-step refinement) can further enhance the accuracy of community label recovery beyond that of the one-step procedure. This motivates the design of Algorithm 3, which builds on Algorithm 2 by incorporating an extra refinement step.

Our work shares similar philosophy with the one-step estimation in the maximum likelihood estimation (Bickel, 1975) and the one-step and two-step local linear approximation solutions in folded concave penalized estimation (Fan et al., 2014). Theorem 3 provides a theoretical justification for Algorithm 3: compared to the one-step refinement, the two-step refinement significantly accelerates the convergence rate of the clustering error. When the

sample size n is large, the effect is negligible; however, for smaller n , the improvement becomes substantial, which is consistent with the simulation results in Section 5.2.

4 Theoretical Properties

This section gives upper bounds on the community labeling error rate for the initialization algorithm TCSC and the refinement algorithm R-TCSC, respectively.

The following assumptions ensure that the true labels $\mathbf{c}^* \in [K]^n$ are estimable. Recall that $n_k(\mathbf{c}^*) = \sum_{i=1}^n \mathbb{I}\{\mathbf{c}^*(i) = k\}$, $\forall k \in [K]$. Assumption 1 ensures that the K communities do not degenerate as n grows, i.e., the ratio $n_k(\mathbf{c}^*)/n_l(\mathbf{c}^*)$ does not vanish for any $k, l \in [K]$. This condition is standard in the theoretical works on community detection (see, e.g., Zhang and Zhou (2016); Gao et al. (2018); Yun and Proutiere (2016); Ariu et al. (2023)).

Assumption 1. *There exists a constant $C \geq 1$, such that $\frac{n}{CK} \leq n_k(\mathbf{c}^*) \leq \frac{Cn}{K}$, $\forall k \in [K]$.*

Recall that $\mathbf{\Lambda} = (\lambda_{ik})_{n \times K} \in [0, 1]^{n \times K}$, where λ_{ik} captures the popularity of node i in community k . Suppose $\mathbf{\Lambda} = \rho_n \mathbf{\Lambda}_0$, where $\mathbf{\Lambda}_0 \in (0, 1)^{n \times K}$ is a constant matrix and $\rho_n \in (0, 1]$ is the sparsity parameter, following Chen and Lei (2018). This implies the edge probability matrix $\mathbf{\Theta} = \rho_n^2 \mathbf{\Theta}_0$ for a constant matrix $\mathbf{\Theta}_0$. As ρ_n decreases, connectivity becomes sparser, reducing available information and making community detection more difficult. We relax the conditions from Chen and Lei (2018), which required $n\rho_n^4 \gg (\log n)^2$ and a constant K , to the weaker condition in Assumption 2.

Assumption 2. *The sparsity parameter ρ_n satisfies $n\rho_n^2/K^2 \geq C(\log n)^2$, for a large constant $C > 0$.*

Recall that $\tau_{ij} = 0$ for each i, j with $\mathbf{c}^*(i) \neq \mathbf{c}^*(j)$, and $\tau_{ij} = \left| \frac{D_{\mathbf{P}_{\mathbf{c}^*(i)}}(\boldsymbol{\lambda}_i, \boldsymbol{\lambda}_j)}{D_{\mathbf{P}_{\mathbf{c}^*(i)}}^{1/2}(\boldsymbol{\lambda}_i, \boldsymbol{\lambda}_i) D_{\mathbf{P}_{\mathbf{c}^*(i)}}^{1/2}(\boldsymbol{\lambda}_j, \boldsymbol{\lambda}_j)} \right|$ for each i, j with $\mathbf{c}^*(i) = \mathbf{c}^*(j)$ as shown in Corollary 1. Accordingly, we impose the following assumptions on $\{\tau_{ij}\}_{i,j \in [n]}$ to ensure that nodes within the same community remain sufficiently similar to be reliably identified.

Assumption 3. *For each $i \in [n]$, define $\mathcal{G}_i = \{j \in [n] : \mathbf{c}^*(j) = \mathbf{c}^*(i), |\tau_{ij}| \geq \phi_{1,n}\}$, for a sequence $\phi_{1,n} \in (0, 1]$. Let $\mathcal{H} = \{i \in [n] : |\mathcal{G}_i| \geq n_{\mathbf{c}^*(i)}(\mathbf{c}^*)(1 - \tilde{\eta}_{n,0})\}$ and $\bar{\mathcal{H}} = [n] \setminus$*

\mathcal{H} . Assume that $|\bar{\mathcal{H}}| \leq \tilde{\eta}_{n,1}n$, for two sequences $\tilde{\eta}_{n,1} = o((n\rho_n^2)^{-1}(\log n)^2)$ and $\tilde{\eta}_{n,0} = o((n\rho_n^2)^{-1/2} \log n)$.

Note that \mathcal{G}_i in Assumption 3 can be written as $\{j \in [n] : \mathbf{c}^*(j) = \mathbf{c}^*(i), |\cos(\boldsymbol{\xi}_i, \boldsymbol{\xi}_j)| \geq \phi_{1,n}\}$, meaning that a major portion of node pairs within the same community occupy non-orthogonal positions in the eigenspace (i.e., $\boldsymbol{\xi}_i, \boldsymbol{\xi}_j$). The set \mathcal{H} consists of nodes with relatively clear community signals, generally aligned with a major subset of their peers, while the small size of $\bar{\mathcal{H}}$ allows for a few nodes to have weak or ambiguous affiliations.

Assumption 4. Let $\mathcal{I} = \{i \in [n] : D_{\mathbf{P}_{\mathbf{c}^*(i)}}^{1/2}(\boldsymbol{\lambda}_i, \boldsymbol{\lambda}_i) \geq \phi_{2,n}\}$ for a sequence $\phi_{2,n}$. Assume that $|\mathcal{I}| > n(1 - \tilde{\eta}_{n,2})$ for some $\tilde{\eta}_{n,2} = o((\log n)^2(n\rho_n^2)^{-1})$, and $\max_{i \in [n]} D_{\mathbf{P}_{\mathbf{c}^*(i)}}(\boldsymbol{\lambda}_i, \boldsymbol{\lambda}_i) \lesssim K^2/n$.

Note that $D_{\mathbf{P}_{\mathbf{c}^*(i)}}^{1/2}(\boldsymbol{\lambda}_i, \boldsymbol{\lambda}_i) = \|\boldsymbol{\xi}_i\|$, so \mathcal{I} in Assumption 4 can be written as $\{i \in [n] : \|\boldsymbol{\xi}_i\| \geq \phi_{2,n}\}$. This ensures that the eigenvector rows retain sufficient information to capture the spatial positions of the nodes. Moreover, the condition $\max_{i \in [n]} D_{\mathbf{P}_{\mathbf{c}^*(i)}}(\boldsymbol{\lambda}_i, \boldsymbol{\lambda}_i) \lesssim K^2/n = \|\Xi\|_{\text{F}}^2/n$ is well justified: in SBM, [Lei and Rinaldo \(2015\)](#) showed that $\|\mathbf{U}_i\|^2 \asymp K/n = \|\mathbf{U}\|_{\text{F}}^2/n$ under Assumption 1, where $\mathbf{U}\mathbf{T}\mathbf{U}^\top$ is the eigendecomposition of its $\mathbb{E}\mathbf{A}$, and \mathbf{U}_i denotes its i -th row.

We now present an upper bound on the error rate of the TCSC in Theorem 1.

Theorem 1 (Error Rate of the TCSC). Assume that $\boldsymbol{\Theta}$ has K^2 nonzero singular values $\sigma_{1,n} \geq \dots \geq \sigma_{K^2,n}$, with $\sigma_{1,n}/\sigma_{K^2,n} \leq C_1\sqrt{\log n}$ for some constant $C_1 > 0$. Suppose Assumptions 1-2 hold, and Assumptions 3-4 are satisfied for some $\phi_{1,n}$ and $\phi_{2,n}$ such that, for a large constant $C_2 > 0$,

$$\frac{K}{\sqrt{n}} \gtrsim \phi_{1,n}\phi_{2,n} \geq C_2 \frac{\rho_n K \sqrt{\log n}}{\sigma_{K^2,n}}. \quad (11)$$

If we set $d_n = \phi_{1,n}/2$ in Algorithm 1, there exists a constant $C > 0$ such that

$$\mathbb{P}\left\{\ell(\mathbf{c}^*, \hat{\mathbf{c}}^{(0)}) \leq \tilde{\eta}_n\right\} \geq 1 - Cn^{-4}, \quad (12)$$

for a sequence $\tilde{\eta}_n = o(1)$, and $\hat{\mathbf{c}}^{(0)}$ is the output of Algorithm 1.

Condition (11) holds under mild conditions. Specifically, by the assumptions, we have $\sigma_{1,n} \geq \|\Theta\|_F/K \geq Cn\rho_n^2/K$ and $\sigma_{K^2,n} \geq C\sigma_{K^2,1}/\sqrt{\log n} \geq Cn\rho_n^2/(K\sqrt{\log n})$. Together with Assumption 2, we can obtain $\rho_n K\sqrt{\log n}/\sigma_{K^2,n} \lesssim (K/\sqrt{n})\{K \log n/(n\rho_n^2)^{1/2}\} \leq CK/\sqrt{n}$ for some small constant $C > 0$.

Theorem 1 establishes that Algorithm 1 yields a weakly consistent estimator of \mathbf{c}^* under mild conditions. Next, we will show that applying the refinement via Algorithm 2 upgrades this weakly consistent estimator to a strongly consistent one.

To establish strong consistency, we introduce two additional assumptions.

Assumption 5. *For each $l \in [K]$ and all distinct $k, k' \in [K]$ with $k \neq k'$, the popularity vectors satisfy that $|\cos(\boldsymbol{\lambda}^{(l,k)}, \boldsymbol{\lambda}^{(l,k')})| \leq 1 - \delta$ for some constant $\delta > 0$.*

Assumption 5 ensures the detectability of the true community labels \mathbf{c}^* . Similar assumptions are standard in the PABM literature—for instance, Noroozi et al. (2021b) require the set $\{\boldsymbol{\lambda}^{(k,l)}\}_{l \in [K]}$ to be linearly independent for each $k \in [K]$. Notably, we can allow δ to approach zero at a certain rate, which just requires strengthening other assumptions.

Intuitively, the success of Algorithm 2 depends on the quality of the initial estimates. The initialization must provide a reasonably accurate starting point. We show that a weakly consistent initial estimator satisfying a mild error condition is sufficient, provided Assumptions 2–4 are moderately strengthened. Under this condition, the refinement procedure in Algorithm 2 substantially reduces the error rate. We formalize these strengthened conditions in Assumption 6.

Assumption 6. *(Strengthened Assumption 2).*

$$\frac{K \log n}{n\rho_n^4} = o(1) \text{ and } K \leq n^{1/6}. \quad (13)$$

(Strengthened Assumptions 3 and 4). $\tilde{\eta}_{n,1}, \tilde{\eta}_{n,2} = o(1) \min\{(n\rho_n^2)^{-1}(\log n)^2, \rho_n^4/K^2\}$, and $\tilde{\eta}_{n,0} = o(1) \min\{(n\rho_n^2)^{-1/2} \log n, \rho_n^4/K\}$.

The strengthened assumptions remain quite mild. For instance, under the PABM, Chen and Lei (2018) required $n\rho_n^4 \gg (\log n)^2$ with fixed K , while Noroozi et al. (2021b) showed

in their Corollary 1 that for $K = 2$, weak consistency of their community label estimator requires $n\rho_n^6 \rightarrow \infty$.

We then show that a strongly consistent estimate of the community label vector \mathbf{c}^* can be obtained via one-step R-TCSC in Theorem 2.

Theorem 2 (Error Rate of the One-Step R-TCSC). *If Assumptions 1, 5 and 6 hold, then there exist positive constants C_1 and C_2 such that*

$$\mathbb{P} \left\{ \bigcup_{\pi: [K] \rightarrow [K]} \left(\hat{\mathbf{c}}^{(1)} = \pi[\mathbf{c}^*] \right) \right\} > 1 - C_1 n^{-(1+C_2)}, \quad (14)$$

where $\hat{\mathbf{c}}^{(1)}$ is the output of Algorithm 2, and $\pi[\mathbf{c}^*] = (\pi(\mathbf{c}^*(1)), \dots, \pi(\mathbf{c}^*(n)))^\top$.

Theorem 2 establishes that the one-step R-TCSC refines the weakly consistent estimate of the community label vector \mathbf{c}^* into a strongly consistent one, achieving exact recovery with high probability. And all the simulation results in Section 5.1 is consistent it.

However, as shown in Section 3.3, two-step refinement provides additional benefits when the number of nodes n is small, motivating a theoretical investigation of Algorithm 3. In fact, it follows from the proof of Theorem 2 that

$$\mathbb{P} \left\{ n\ell(\mathbf{c}^*, \hat{\mathbf{c}}^{(1)}) = o(1) \right\} \geq 1 - C_1 n^{-(1+C_2)},$$

for two constants $C_1, C_2 > 0$, as $n \rightarrow \infty$. We then show the two-step R-TCSC achieves an additional gain in convergence rate over the one-step R-TCSC in Theorem 3.

Theorem 3 (Additional gain in convergence rate of the Two-Step R-TCSC). *Under the conditions of Theorem 2, there exist constants C and $C' > 0$ such that*

$$\mathbb{P} \left\{ \ell(\mathbf{c}^*, \hat{\mathbf{c}}^{(2)}) = o\left(\frac{1}{n\rho_n^2}\right) \right\} > 1 - C n^{-(1+C')}, \quad (15)$$

where $\hat{\mathbf{c}}^{(2)}$ denote the outputs of Algorithm 3, and there exist a constant $C_0 > 0$ such that

$$\mathbb{P} \left\{ \bigcap_{t=1,2} \left(\frac{\ell(\mathbf{c}^*, \hat{\mathbf{c}}^{(t)})}{\ell(\mathbf{c}^*, \hat{\mathbf{c}}^{(t-1)})} < \frac{C_0}{n\rho_n^2} \right) \right\} > 1 - C n^{-(1+C')}, \quad (16)$$

where $\hat{\mathbf{c}}^{(0)}$, $\hat{\mathbf{c}}^{(1)}$ and $\hat{\mathbf{c}}^{(2)}$ denote the outputs of Algorithms 1, 2, and 3, respectively.

As $n \rightarrow \infty$, $n\ell(\mathbf{c}^*, \hat{\mathbf{c}}^{(1)}) = o(1) < 1$ guarantees the strong consistency of the one-step refinement. However, when n is finite, the convergence rate implied by $o(1)$ may be insufficiently fast, whereas $\ell(\mathbf{c}^*, \hat{\mathbf{c}}^{(2)}) = o(1/(n\rho_n^2))$ represents a much faster rate. In particular, when ρ_n is fixed, we have $\ell(\mathbf{c}^*, \hat{\mathbf{c}}^{(2)}) = o(1/n)$. This explains why two-step refinement can lead to additional gains when n is small, while the improvement over one-step refinement becomes negligible as n increases, as corroborated by the empirical results presented in Section 5.2. Thus, to accommodate small-sample settings, we employ the two-step R-TCSC algorithm in all simulation studies and real-data analyses. Moreover, inequality (16) indicates that the clustering error rate decreases monotonically and geometrically with each refinement step ($t = 1, 2$), which is also consistent with the simulation results in Section 5.2, where the first refinement step yields a larger error reduction than the second refinement step when n is not so large.

5 Simulation Study

In this section, we compare the performance of the proposed TCSC and R-TCSC against several competitors: EP that optimizes the likelihood modularity under the PABM (Chen and Lei, 2018), SSC-A that uses using the rows of \mathbf{A} (Noroozi et al., 2021b), and OSC, SSC-ASE (Koo et al., 2023) that use the spectral embedding of \mathbf{A} . For EP, since only the algorithm for $K = 2$ is provided by Chen and Lei (2018), we compare with it only in case $K = 2$. For the other competing methods, we use the publicly available source code from Koo et al. (2023), following their recommended configurations and default settings. To adaptively select the threshold d_n in Algorithm 1, we compute all values $(\hat{\tau}_{ij})_{1 \leq i < j \leq n}$ and choose the point of the steepest drop in their frequency histogram as the threshold. We use the two-step R-TCSC, Algorithm 3. Furthermore, in practice, we replace $\bar{\mathbf{A}}_{-i}^{(k,l)}(\hat{\mathbf{c}}^{(t)})$ with $\bar{\mathbf{A}}^{(k,l)}(\hat{\mathbf{c}}^{(t)})$ in (9) and (10) for efficiency, as the difference is negligible.

5.1 Comparison of Basic Settings

To compare the effectiveness of different methods, we use the community detection error defined in (2). We consider the settings with $n = 128, 256, 512, 1024$ nodes and $K = 2, 3, 4$ communities, and each experiment is repeated 100 times. In each simulation, community labels $\mathbf{c}^*(1), \dots, \mathbf{c}^*(n)$ are drawn *i.i.d.* from a multinomial distribution with parameters $\{1, (\pi_1, \dots, \pi_K)^\top\}$. The popularity vectors $\{\boldsymbol{\lambda}^{(k,l)}\}_{k,l \in [K]}$ are sampled from two different joint distributions, depending on whether $k = l$ or $k \neq l$. The edge probability matrix $\Theta = (\theta_{ij})_{n \times n}$ is constructed as $\theta_{ij} = \lambda_{i\mathbf{c}^*(j)} \lambda_{j\mathbf{c}^*(i)}$, the upper triangular entries of the adjacency matrix $(A_{ij})_{1 \leq i < j \leq n}$ are independently drawn from $\text{Bernoulli}(\theta_{ij})$, and the full adjacency matrix is obtained by symmetrization and $A_{ii} = 0$.

First, we consider the case where community sizes are balanced: $\pi_k = 1/K$ for $k \in [K]$. The popularity parameters are generated as follows: intra-community parameters $\boldsymbol{\lambda}^{(k,k)} \stackrel{\text{iid}}{\sim} \text{Beta}(2, 1)$ and inter-community parameters $\boldsymbol{\lambda}^{(k,l)} \stackrel{\text{iid}}{\sim} \text{Beta}(1, 2)$ for $k \neq l \in [K]$. Figure 3 presents the results for community detection under balanced community sizes, where the vertical axis shows the proportion of misclustered nodes as defined in (2). The figure illustrates two key findings: (i) the error rates of both TCSC and R-TCSC decrease as n increases, consistent with Theorems 1 and 3; (ii) across all settings, TCSC and R-TCSC outperform competing methods, with R-TCSC rapidly converging to zero error.

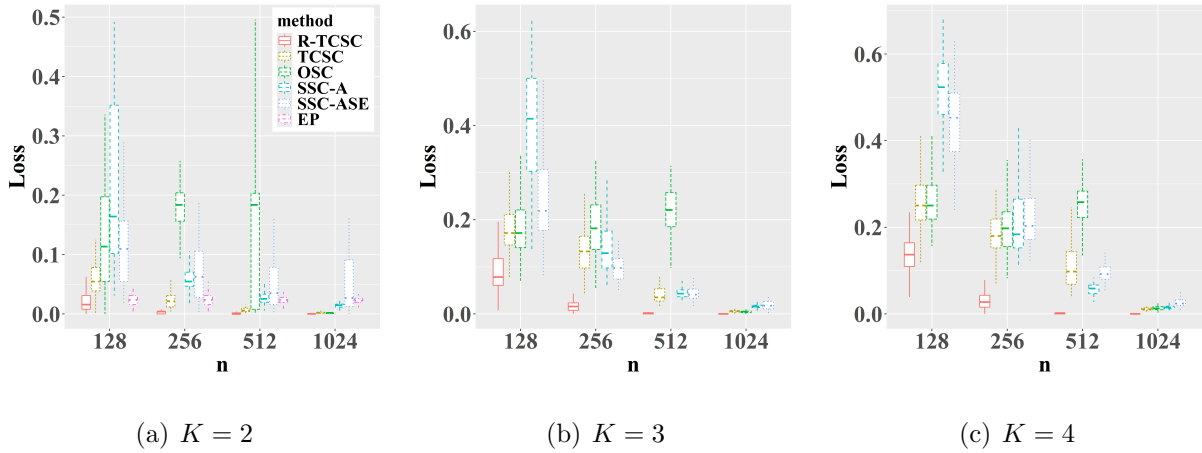


Figure 3: Comparison of community detection performance under balanced communities.

Second, we consider the case of imbalanced community sizes: $\pi_k = k^{-1}/(\sum_{\ell=1}^K \ell^{-1})$ for $k \in [K]$. The popularity parameters are generated as in the balanced setting. The community detection results, shown in Figure 4, lead to two main observations: (i), similar to the balanced case (Figure 3), both TCSC and R-TCSC outperform competing methods under imbalanced settings; (ii) by comparing the results to $K = 3, 4$, and $n = 1024$ across the two figures (Figures 3 and 4), we observe that R-TCSC exhibits more stable performance than the other methods as community sizes become more imbalanced.

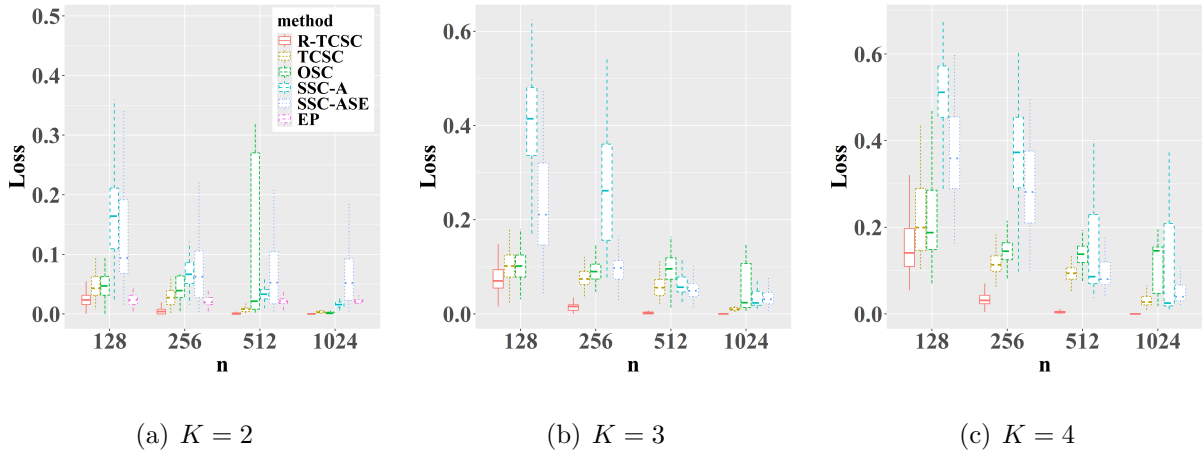


Figure 4: Comparison of community detection performance under imbalanced communities.

Third, we consider the disassortative case, where intra-community popularity parameters are weaker than inter-community popularity parameters. Specifically, the popularity parameters are generated as follows: $\lambda^{(k,k)}$ are drawn independently from Beta(1, 2) and $\lambda^{(k,l)}$ for $k \neq l \in [K]$ are drawn independently from Beta(2, 1). As shown in Figure 5, R-TCSC maintains strong and stable performance even in the disassortative case.

To further examine how various methods respond to assortative versus disassortative structures, we fix $n = 512$ and systematically vary the degree of assortativity. Specifically, within-community popularity parameters $\lambda^{(k,k)}$, are drawn *i.i.d.* from Beta($x, 3 - x$), while between-community parameters $\lambda^{(k,l)}$ are drawn *i.i.d.* from Beta($3 - x, x$) for $k \neq l \in [K]$, and let $x = 0.5, 1, 1.5, 2, 2.5$. When $x = 0.5$ or 1, the model exhibits expected disassortative behavior. When $x = 2$ or 2.5, it becomes assortative. The case $x = 1.5$ corresponds to a setting where, in expectation, within- and between-community popularity are equal,

making label recovery particularly challenging. The results for community detection are presented in Figure 6. When $x = 1.5$ (the theoretically most difficult case, where within- and between-community popularity are equal in expectation), SSC-A performs poorly and nearly fails, and although EP had been consistently stable under $K = 2$, it also shows signs of deterioration. In contrast, R-TCSC remains consistently strong across all settings. Although TCSC trails R-TCSC, it consistently ranks as one of the top-performing methods.

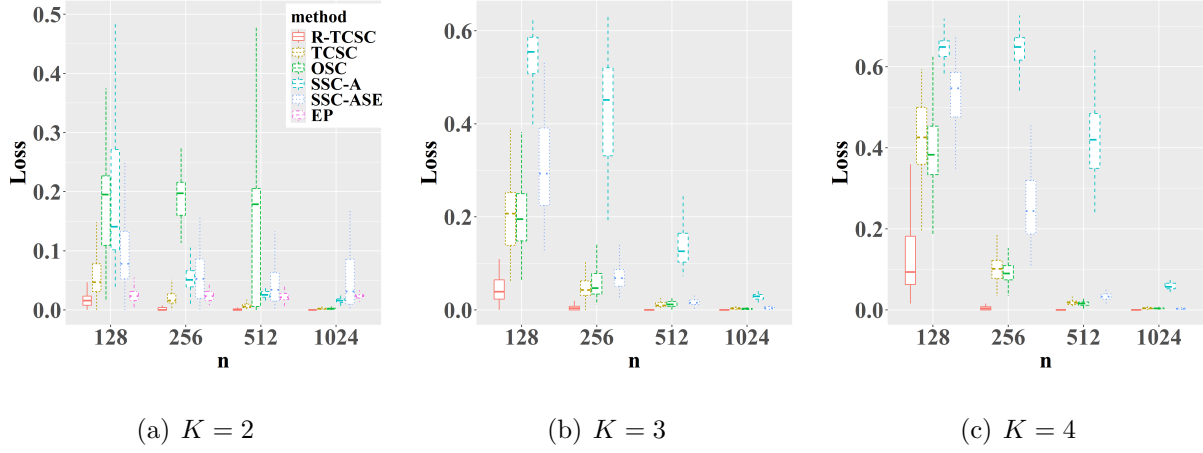


Figure 5: Comparison of community detection performance under disassortative models.

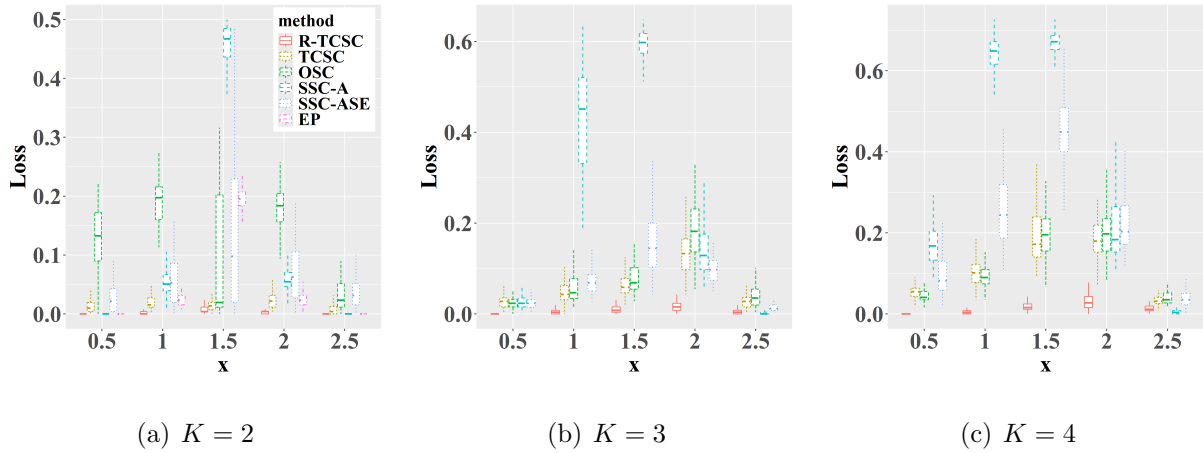


Figure 6: The community detection performance from disassortative to assortative.

5.2 Comparison of one-step and two-step refinements

Following the numerical simulation setup outlined in Section 5.1, we compared the performance of Algorithm 2, the one-step R-TCSC (abbreviated as R-TCSC-1), and Algorithm 3, the two-step R-TCSC (abbreviated as R-TCSC-2), relative to the initialization algorithm TCSC. Simulation results demonstrate that R-TCSC-1 achieves substantial improvements over the initialization. When the number of nodes is large (e.g., $n = 1024$), R-TCSC-1 and R-TCSC-2 perform similarly, with the second refinement step providing negligible additional gains. In contrast, when n is small (e.g., $n = 128$ or 256), the second refinement step further enhances performance. Consequently, we employ R-TCSC-2 throughout the main text and refer to it as R-TCSC for simplicity.

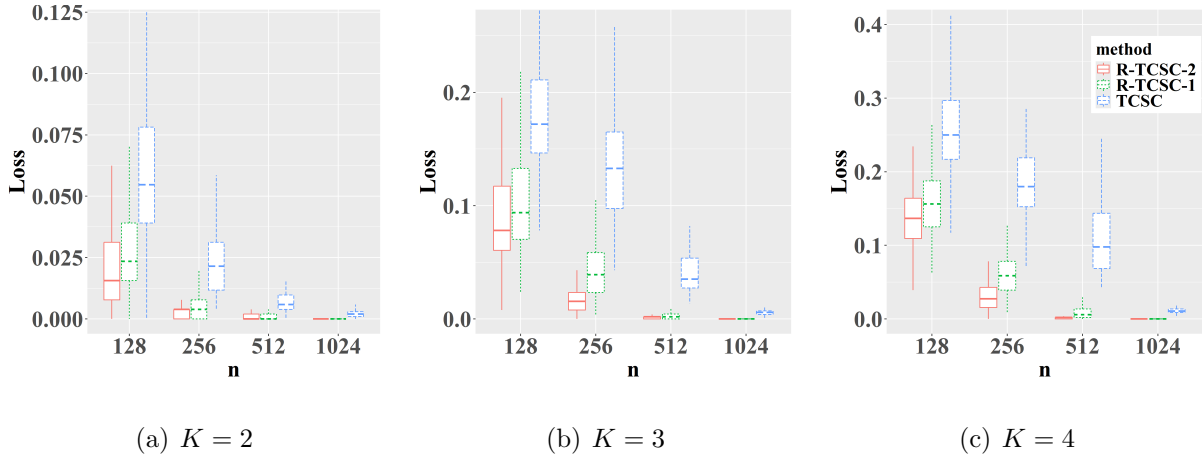


Figure 7: R-TCSC-1 vs R-TCSC-2 in case of balanced communities.

5.3 Heterogeneity within-community

In this section, we consider the case of within-community heterogeneity. In previous settings, $(\lambda_{i1}, \dots, \lambda_{iK})_{i, c^*(i)=k}$ were assumed to be *i.i.d.*, a key assumption underlying the theoretical guarantees of OSC. Here, we relax this to independent but non-identically distributed (non-*i.i.d.*) samples and show that under this setting, the performance of OSC deteriorates significantly. To introduce heterogeneity, for each $k, l \in [K]$, we generate the first half of the entries in $\boldsymbol{\lambda}^{(k,l)}$ *i.i.d.* from $\text{Beta}(x, 2)$ with $x = 4, 8, 12, 16, 20$, and the sec-

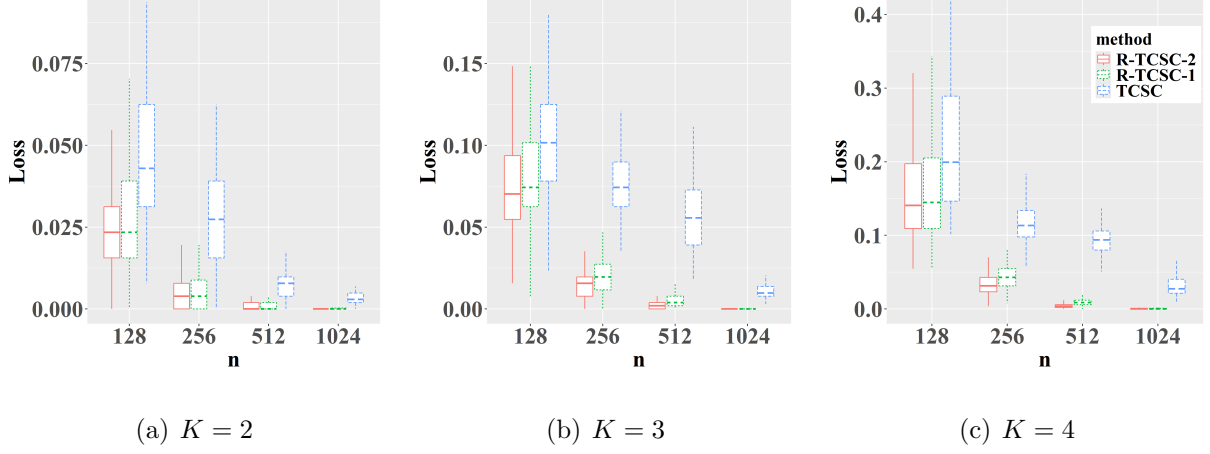


Figure 8: R-TCSC-1 vs R-TCSC-2 in case of unbalanced communities.

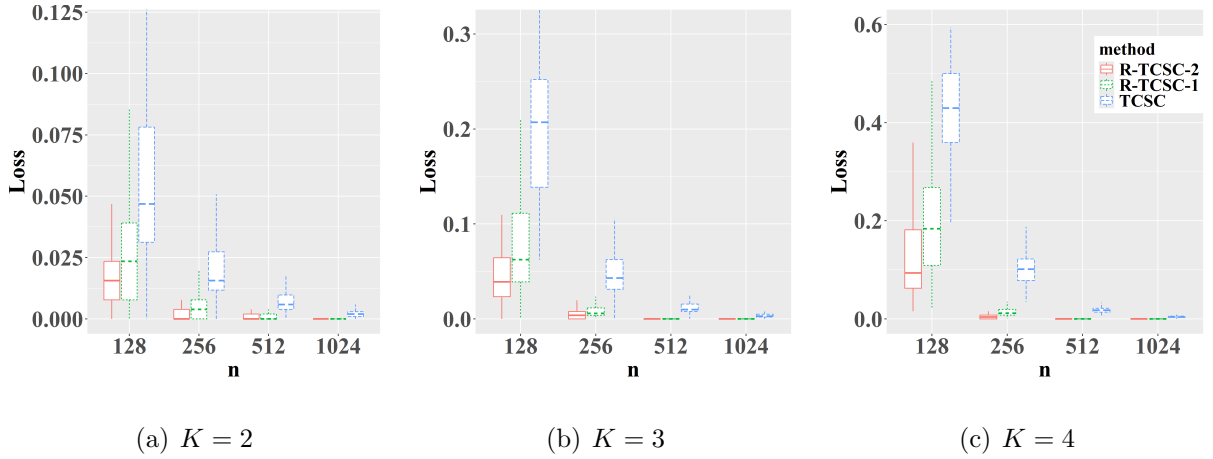


Figure 9: R-TCSC-1 vs R-TCSC-2 in case of disassortative models.

and half *i.i.d.* drawn from $\text{Beta}(1, 1)$. Figure 10 presents the community detection results with $n = 512$. As x increases, the Hellinger distance between $\text{Beta}(x, 2)$ and $\text{Beta}(1, 1)$, used for the first and second halves of $\boldsymbol{\lambda}^{(k,l)}$, grows larger: 0.35, 0.52, 0.61, 0.66, 0.70. Correspondingly, the performance of the OSC algorithm deteriorates noticeably with increasing heterogeneity.

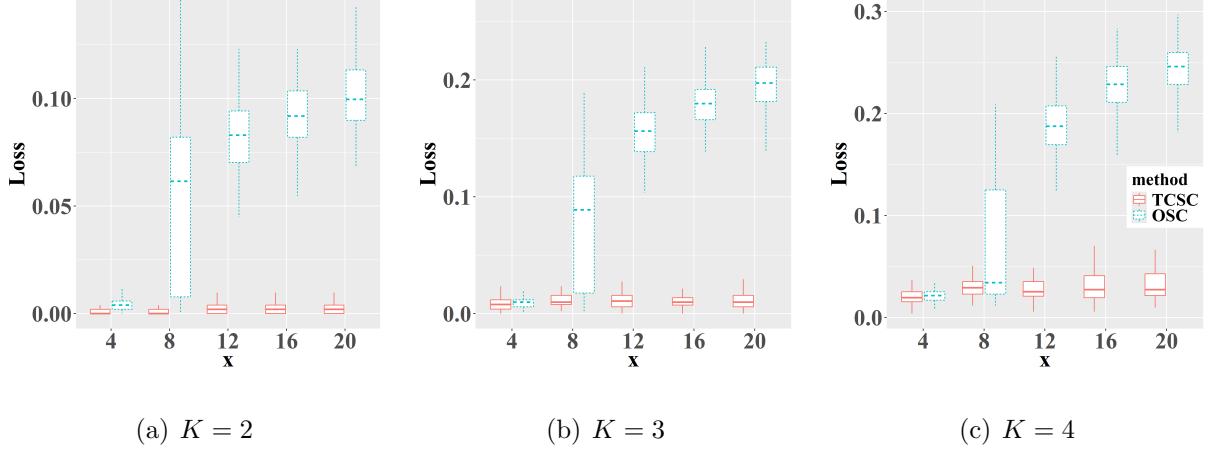


Figure 10: The community detection performance when $(\lambda_{i1}, \dots, \lambda_{iK})_{i:c^*(i)=k}$ for nodes in the same community are drawn independently from heterogeneous distributions.

6 Selection of the Number of Communities

Until now, we have assumed that the number of communities K is known. However, in practice, this is typically unknown. It is an important research topic to choose the number of communities in network data, such as those for SBM (Saldana et al., 2017; Chen and Lei, 2018; Li et al., 2020). To the best of our knowledge, the only method for estimating K under the PABM is proposed by Noroozi et al. (2021b), which selects K by minimizing the squared loss with a penalty term, denoted as LP. We propose a new approach to estimate K by leveraging the structure of Θ in (3), which implies that $\text{rank}(\Theta^{(k,k)}(\mathbf{c}^*)) = 1$ for any $k \in [K]$. Define

$$\mathbf{c}_{\tilde{K}} \in \arg \min_{\substack{\tilde{\mathbf{c}} \in [\tilde{K}]^n, \forall k \in [\tilde{K}], \\ n_k(\tilde{\mathbf{c}}) \in \left[\frac{n}{C\tilde{K}}, \frac{Cn}{\tilde{K}}\right]}} f(\tilde{\mathbf{c}}, \Theta), \quad (17)$$

for $\tilde{K} \in [K_{\max}]$, where $f(\tilde{\mathbf{c}}, \Theta) = \max_{k \in [\tilde{K}]} \sigma_2(\Theta^{(k,k)}(\tilde{\mathbf{c}}))$ and $\Theta^{(k,k)}(\tilde{\mathbf{c}}) = (\theta_{ij})_{i,j:\tilde{\mathbf{c}}(i)=\tilde{\mathbf{c}}(j)=k}$.

The following proposition shows that $f(\mathbf{c}_{\tilde{K}}, \Theta)$ attains its minimum at the true number of communities K . Furthermore, replacing Θ with the observed adjacency matrix \mathbf{A} , the empirical version $f(\mathbf{c}_{\tilde{K}}, \mathbf{A})$ continues to identify K accurately with high probability.

Proposition 2. *Suppose that, for each $\tilde{K} < K$, $f(\mathbf{c}_{\tilde{K}}, \Theta) \geq Cn\rho_n^2/(\tilde{K}\sqrt{\log n})$ for a constant $C > 0$. Then, we have the following results:*

(I) If $\tilde{K} \geq K$, $f(\mathbf{c}_{\tilde{K}}, \boldsymbol{\Theta}) \equiv 0$;

(II) When $K_{\max} \leq n^{1-C}$ for a constant $C > 0$ and $\rho_n^2 n / K_{\max} \gg (\log n)^2$, then,

$$\begin{cases} f(\mathbf{c}_{\tilde{K}}, \mathbf{A}) \lesssim \rho_n \sqrt{\frac{n}{\tilde{K}}}, & K \leq \tilde{K} \leq K_{\max}; \\ \frac{n\rho_n^2}{\tilde{K}\sqrt{\log n}} \lesssim f(\mathbf{c}_{\tilde{K}}, \mathbf{A}) \lesssim \frac{n\rho_n^2}{\tilde{K}}, & \tilde{K} < K, \end{cases} \quad (18)$$

holds with probability at least $1 - n^{-C'}$ for a constant $C' > 0$.

Remark 1. The assumption of Proposition 2 ensures the identification of the community number K by providing the necessary conditions for the correct estimation of K . This assumption is not restrictive. Taking $K = 2$ as an example, it holds under the conditions of Theorem 1. Specifically, for $\tilde{K} < K$, $f(\mathbf{c}_{\tilde{K}}, \boldsymbol{\Theta}) = \sigma_2(\boldsymbol{\Theta}) \geq C\sigma_1(\boldsymbol{\Theta})/\sqrt{\log n} \geq C\|\boldsymbol{\Theta}\|_F/(2\sqrt{\log n}) \gtrsim n\rho_n^2/\sqrt{\log n}$.

Assume $2 \leq K \leq K_{\max}$ for some integer $K_{\max} > 1$. We estimate K by

$$\hat{K}(\mathbf{c}_{\tilde{K}}) = \arg \max_{\tilde{K} \in \{2, \dots, K_{\max}\}} \frac{f(\mathbf{c}_{\tilde{K}-1}, \mathbf{A})}{f(\mathbf{c}_{\tilde{K}}, \mathbf{A}) + \log n}. \quad (19)$$

The addition of the $\log n$ penalty follows the same reasoning as in Yu et al. (2022) for selecting the number of factors in the factor model. Specifically, it prevents overestimation of K by offsetting the rapid decay of $f(\mathbf{c}_{\tilde{K}}, \mathbf{A})$ when $\tilde{K} > K$.

By Proposition 2, we directly obtain the following corollary.

Corollary 2. Under the assumptions of Proposition 2, we have $\hat{K}(\mathbf{c}_{\tilde{K}}) = K$ holds with probability at least $1 - n^{-C}$ for a constant $C > 0$.

Building on Corollary 2, we transform the problem (19) into the following form:

$$\hat{K} = \arg \max_{\tilde{K} \in \{2, \dots, K_{\max}\}} \frac{f(\mathbf{c}_{\tilde{K}-1}, \mathbf{A})}{\frac{1}{d} \sum_{K'=\tilde{K}}^{\tilde{K}+d-1} f(\mathbf{c}_{K'}, \mathbf{A}) + \log n}, \quad (20)$$

where d is the window width parameter. While $d = 1$ suffices theoretically, we set $d = 2$ throughout for improved robustness in practice. We use TCSC to estimate $\mathbf{c}_{\tilde{K}}$ in (20), since the K-means step in TCSC tends to favor more balanced community sizes, which aligns better with the structure assumed in the optimization of (17). As a result, we refer to the proposed method as SVCP (Singular Value Change Point).

Table 2: Accuracy of SVCP and LP in selecting the number of communities K .

Method	$K = 2$	3	4	5	6	7	8
LP(Noroozi et al., 2021b)	0.92	1.00	1.00	0.99	0.63	0.76	0.04
SVCP (our method)	0.92	1.00	1.00	0.99	0.87	1.00	0.93

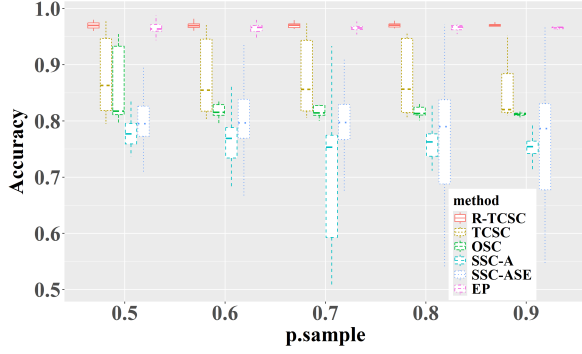
To examine the numerical performance of SVCP against LP, we consider following simulation setup: number of nodes $n = 512$; number of communities, $K = 2, 3, 4, 5, 6, 7, 8$; community size parameters, $\pi_k = 1/K$ for $k = 1, \dots, K$; intra-community parameters $\boldsymbol{\lambda}^{(k,k)} \stackrel{\text{iid}}{\sim} \text{Beta}(2, 1)$ and inter-community parameters $\boldsymbol{\lambda}^{(k,l)} \stackrel{\text{iid}}{\sim} \text{Beta}(1, 2)$ for $k \neq l \in [K]$. Both LP and SVCP achieve comparable performance when K is small, but SVCP shows a clear advantage as K increases, as shown in Table 2. Since $n = 512$ is fixed, increasing K raises model complexity and the difficulty of estimating K . Table 2 indicates that LP starts to fail when $K = 6, 7$ or 8 , whereas SVCP remains robust.

7 Real Applications

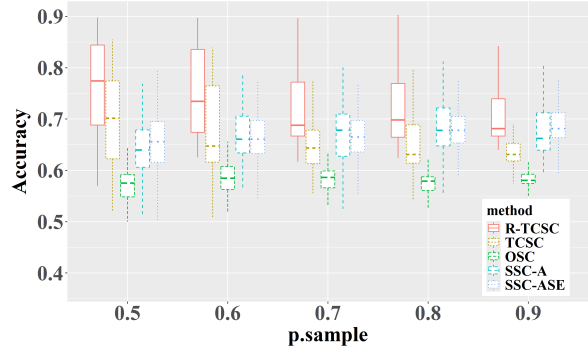
In this section, we analyze two real-world networks with known community labels. We first estimate the number of communities using the method from Subsection 6 and then compare the performance of our proposed TCSC and R-TCSC against baseline methods EP, SSC-A, OSC and SSC-ASE, using the same implementation settings as in Section 5.

To assess both stability and performance, we repeatedly subsample each community in the original network \mathbf{A} by independently selecting nodes with probability $p_{\text{sample}} \in \{0.5, 0.6, 0.7, 0.8, 0.9\}$. After removing isolated nodes (those with degree zero), we obtain a pruned network $\mathbf{A}_{\text{sample}}$. This process is repeated 100 times, allowing us to evaluate the consistency of each community detection method across different subsampled networks.

Digital Bibliography & Library Project (DBLP) Network. The DBLP network extracted by Gao et al. (2009) and Ji et al. (2010), represents authors as nodes, with an edge connecting any pair who attended the same conference. Following Sengupta and Chen (2017), we focus on authors in two research areas: databases and information retrieval.



(a) DBLP Network



(b) Butterfly Network

Figure 11: Community detection performance on two real-world networks

The resulting network contains 2,203 nodes and 1,148,044 edges. We apply the SVCP to estimate the number of communities, obtaining $\hat{K} = 2$, which matches the ground truth. Figure 11 reports clustering accuracy (i.e., $1 - \ell(\mathbf{c}^*, \hat{\mathbf{c}})$), and Figure 11(a) shows that R-TCSC and EP consistently outperform others in both accuracy and robustness.

Butterfly Network. This network, based on the Leeds butterfly dataset (Wang et al., 2018), represents species as nodes and draws edges between visually similar pairs. Following Noroozi et al. (2021b) and Koo et al. (2023), we analyze a subnetwork with 373 nodes and 20,566 edges, comprising the four largest species categories. The PABM is well-suited for this data, as species may resemble others outside their category. Using our proposed SVCP method, we estimated $\hat{K} = 4$, correctly recovering the true number of communities. As shown in Figure 11(b), R-TCSC outperforms all competing methods.

8 Conclusion

The Popularity Adjusted Block Model (PABM) captures heterogeneous node popularity across communities but introduces significant estimation challenges due to its complexity. To address these challenges in this paper, we first propose an effective spectral clustering algorithm, TCSC, and establish its weak consistency under the PABM. We then show that the proposed one-step refinement algorithm, R-TCSC, achieves strong consistency,

and further provide a theoretical guarantee that the two-step refinement accelerates the convergence rate of the clustering error in finite samples. We also introduce a data-driven method for selecting the number of communities, which outperforms existing approaches. Beyond these results, our framework is broadly applicable. It relies only on first-order moment information, avoiding likelihood-based assumptions, and is well suited to general network settings. While our refinement procedure uses spectral clustering for initialization, it can readily incorporate other fast and reliable methods for a wide range of applications.

References

- Abbe, E. and Sandon, C. (2015). Community detection in general stochastic block models: Fundamental limits and efficient algorithms for recovery. In *2015 IEEE 56th Annual Symposium on Foundations of Computer Science*, page 670–688, Berkeley. IEEE Computer Society.
- Agarwal, A. and Xue, L. (2020). Model-based clustering of nonparametric weighted networks with application to water pollution analysis. *Technometrics*, 62(2):161–172.
- Amini, A. A., Chen, A., Bickel, P. J., and Levina, E. (2013). Pseudo-likelihood methods for community detection in large sparse networks. *The Annals of Statistics*, 41(4):2097–2122.
- Ariu, K., Proutiere, A., and Yun, S.-Y. (2023). Instance-optimal cluster recovery in the labeled stochastic block model. *arXiv*, page 2306.12968.
- Bickel, P. J. (1975). One-step huber estimates in the linear model. *Journal of the American Statistical Association*, 70(350):428–434.
- Chen, K. and Lei, J. (2018). Network cross-validation for determining the number of communities in network data. *Journal of the American Statistical Association*, 113(521):241–251.
- Chen, Q., Agarwal, A., Fong, D. K., DeSarbo, W. S., and Xue, L. (2024). Model-based

- co-clustering in customer targeting utilizing large-scale online product rating networks. *Journal of Business & Economic Statistics*, pages 1–13.
- Erdős, P. and Rényi, A. (1959). On random graphs *I*. *Publicationes Mathematicae Debrecen*, 6:290–297.
- Fan, J., Xue, L., and Zou, H. (2014). Strong oracle optimality of folded concave penalized estimation. *The Annals of Statistics*, 42(3):819–849.
- Fortunato, S. (2010). Community detection in graphs. *Physics Reports*, 486(3):75–174.
- Fortunato, S. and Hric, D. (2016). Community detection in networks: A user guide. *Physics Reports*, 659:1–44.
- Gao, C., Ma, Z., Zhang, A., and Zhou, H. (2017). Achieving optimal misclassification proportion in stochastic block model. *Journal of Machine Learning Research*, 18:1–45.
- Gao, C., Ma, Z., Zhang, A. Y., and Zhou, H. H. (2018). Community detection in degree-corrected block models. *The Annals of Statistics*, 46(5):2153–2185.
- Gao, J., Liang, F., Fan, W., Sun, Y., and Han, J. (2009). Graph-based consensus maximization among multiple supervised and unsupervised models. In *Advances in Neural Information Processing Systems*, page 585–593, New York. Curran Associates Inc.
- Goldenberg, A., Zheng, A. X., Fienberg, S. E., and Airoldi, E. M. (2010). A survey of statistical network models. *Foundations and Trends in Machine Learning*, 2(2):129–233.
- Holland, P. W., Laskey, K. B., and Leinhardt, S. (1983). Stochastic blockmodels: First steps. *Social Networks*, 5(2):109–137.
- Hu, J., Zhang, J., Qin, H., Yan, T., and Zhu, J. (2021). Using maximum entry-wise deviation to test the goodness of fit for stochastic block models. *Journal of the American Statistical Association*, 116(535):1373–1382.

- Huang, S., Sun, J., and Feng, Y. (2024). Pcabm: Pairwise covariates-adjusted block model for community detection. *Journal of the American Statistical Association*, 119(547):2092–2104.
- Ji, M., Sun, Y., Danilevsky, M., Han, J., and Gao, J. (2010). Graph regularized transductive classification on heterogeneous information networks. In *Machine Learning and Knowledge Discovery in Databases*, pages 570–586, Berlin. Springer Berlin Heidelberg.
- Jin, J. (2015). Fast community detection by SCORE. *The Annals of Statistics*, 43(1):57–89.
- Jin, J., Ke, Z. T., and Luo, S. (2024). Mixed membership estimation for social networks. *Journal of Econometrics*, 239(2):105369.
- Jin, J., Ke, Z. T., Luo, S., and Wang, M. (2023). Optimal estimation of the number of network communities. *Journal of the American Statistical Association*, 118(543):2101–2116.
- Karrer, B. and Newman, M. E. J. (2011). Stochastic blockmodels and community structure in networks. *Physical Review E*, 83:016107.
- Kim, B., Lee, K. H., Xue, L., and Niu, X. (2018). A review of dynamic network models with latent variables. *Statistics Surveys*, 12:105–135.
- Koo, J., Tang, M., and Trosset, M. W. (2023). Popularity adjusted block models are generalized random dot product graphs. *Journal of Computational and Graphical Statistics*, 32(1):131–144.
- Kumar, A., Sabharwal, Y., and Sen, S. (2004). A simple linear time $(1+\xi)$ -approximation algorithm for k-means clustering in any dimensions. In *45th Annual IEEE Symposium on Foundations of Computer Science*, pages 454–462, Rome. IEEE Symposium on Foundations of Computer Science.
- Lei, J. and Rinaldo, A. (2015). Consistency of spectral clustering in stochastic block models. *The Annals of Statistics*, 43(1):215 – 237.

- Li, T., Levina, E., and Zhu, J. (2020). Network cross-validation by edge sampling. *Biometrika*, 107(2):257–276.
- Moody, J. and White, D. R. (2003). Structural cohesion and embeddedness: A hierarchical concept of social groups. *American Sociological Review*, 68:103–127.
- Noroozi, M., Pensky, M., and Rimal, R. (2021a). Sparse popularity adjusted stochastic block model. *Journal of Machine Learning Research*, 22(193):1–36.
- Noroozi, M., Rimal, R., and Pensky, M. (2021b). Estimation and clustering in popularity adjusted block model. *Journal of the Royal Statistical Society Series B: Statistical Methodology*, 83(2):293–317.
- Rohe, K., Chatterjee, S., and Yu, B. (2010). Spectral clustering and the high-dimensional stochastic blockmodel. *The Annals of Statistics*, 39:1878–1915.
- Saldana, D. F., Yu, Y., and Feng, Y. (2017). How many communities are there? *Journal of Computational and Graphical Statistics*, 26(1):171–181.
- Sengupta, S. and Chen, Y. (2017). A block model for node popularity in networks with community structure. *Journal of the Royal Statistical Society Series B: Statistical Methodology*, 80(2):365–386.
- Spirin, V. and Mirny, L. A. (2003). Protein complexes and functional modules in molecular networks. *Proceedings of the National Academy of Sciences*, 100(21):12123–12128.
- Su, L., Wang, W., and Zhang, Y. (2020). Strong consistency of spectral clustering for stochastic block models. *IEEE Transactions on Information Theory*, 66(1):324–338.
- Sussman, D. L., Tang, M., Fishkind, D. E., and Priebe, C. E. (2011). A consistent adjacency spectral embedding for stochastic blockmodel graphs. *Journal of the American Statistical Association*, 107:1119 – 1128.
- Wang, B., Pourshafeie, A., Zitnik, M., Zhu, J., Bustamante, C., Batzoglou, S., and

- Leskovec, J. (2018). Network enhancement as a general method to denoise weighted biological networks. *Nature Communications*, 9:3108.
- Wang, J., Zhang, J., Liu, B., Zhu, J., and Guo, J. (2020). Fast network community detection with profile-pseudo likelihood methods. *Journal of the American Statistical Association*, 118:1359–1372.
- Wasserman, S. and Faust, K. (1994). *Social Network Analysis: Methods and Applications*. Cambridge University Press, Cambridge.
- Xu, M., Jog, V., and Loh, P. (2020). Optimal rates for community estimation in the weighted stochastic block model. *The Annals of Statistics*, 48(1):183–204.
- Yu, L., He, Y., Kong, X., and Zhang, X. (2022). Projected estimation for large-dimensional matrix factor models. *Journal of Econometrics*, 229(1):201–217.
- Yuan, M., Liu, R., Feng, Y., and Shang, Z. (2022). Testing community structure for hypergraphs. *The Annals of Statistics*, 50(1):147–169.
- Yun, S.-Y. and Proutiere, A. (2016). Optimal cluster recovery in the labeled stochastic block model. In *Advances in Neural Information Processing Systems*, pages 973–981, New York. Curran Associates, Inc.
- Zhang, A. Y. and Zhou, H. H. (2016). Minimax rates of community detection in stochastic block models. *The Annals of Statistics*, 44(5):2252–2280.
- Zhang, J. and Cao, J. (2017). Finding common modules in a time-varying network with application to the drosophila melanogaster gene regulation network. *Journal of the American Statistical Association*, 112(519):994–1008.
- Zhang, J. and Chen, Y. (2017). A hypothesis testing framework for modularity based network community detection. *Statistica Sinica*, 27(1):437–456.
- Zhao, Y., Hao, N., and Zhu, J. (2024). Variational estimators of the degree-corrected latent block model for bipartite networks. *Journal of Machine Learning Research*, 25(150):1–42.

Zhao, Y., Levina, E., and Zhu, J. (2011). Consistency of community detection in networks under degree-corrected stochastic block models. *The Annals of Statistics*, 40:2266–2292.